Morphological and Histological Examination

The degree of lower hind limb necrosis and thigh muscle necrosis was macroscopically evaluated on graded morphological scales (grade 1 to 3) for peripheral tissue damage and muscle necrosis area of the adductor, semimembranous, and medial large muscles. Capillary density of the ischemic hind limb was evaluated by alkaline phosphatase staining, as reported previously.[17] A total of 10 different fields from three different sections were randomly selected, and the number of capillaries was counted under a ×40 objective. Capillary density was expressed as the mean number of capillaries per square millimeter. The number of myofibers in each field was also examined and the capillary/muscle fiber ratio calculated.

Radioimmunoassay for Human AM

Human AM production was examined 1, 2, and 4 weeks after gene transfer in the naked AM group, AM-gelatin group, and control group ($n=5$ each). The muscles were harvested for radioimmunoassay and immunohistochemical examination. Immunoreactive human AM level in rabbit muscles was determined by immunoradiometric assay with the use of a specific kit (Shionogi Co, Ltd).[19] Tissue content of vascular endothelial growth factor (VEGF) was examined by ELISA kit (R&D systems).

Immunohistochemistry for Human AM, Ki67 Antigen, and Phosphorylated Akt

Immunohistochemical studies were performed on formalin-fixed, paraffin-embedded 4-μm sections of ischemic thigh muscles 7 days after gene transfer. To elucidate AM expression after gene therapy, immunohistochemistry for human AM was performed with the use of a monoclonal antibody recognizing AM-(12–25) (1:100), as reported previously.[20] To evaluate the proliferative potential of AM, tissue sections were stained for Ki67, a marker for cell proliferation, with the use of monoclonal anti-Ki67 antibody (1:100) (DAKO). AM has recently been shown to promote proliferation of vascular endothelial cells at least in part through the PI3k/Akt pathway.[21] Thus, immunohistochemistry for phosphorylated Akt was performed with mouse monoclonal anti-phosphorylated Akt antibody (1:100) (Cell Signaling Technology).

Western Blot Analysis

To identify Akt phosphorylation in ischemic muscles after AM gene transfer, Western blotting was performed with the use of a commercially available kit (PhosphoPlus Akt [Ser473] Antibody Kit, Cell Signaling Technology). Ischemic muscles in the 3 groups were obtained 7 days after AM gene transfer. These samples were homogenized on ice in 0.1% Tween 20 homogenization buffer with a protease inhibitor (Complete, Roche). After centrifugation for 20 minutes at 4°C, the supernatant was used for Western blot analysis. The 50 μg of protein was transferred into sample buffer, loaded on 7.5% SDS-polyacrylamide gel, and blotted onto nitrocellulose membrane through the use of a wet blotting system. After blocking for 60 minutes, the membranes were incubated with primary antibodies (1:500) at 4°C overnight. The membranes were then incubated with secondary antibodies, which were conjugated with horseradish peroxidase (Cell Signaling Technology), at a final dilution of 1:2000. Signals were detected through the use of LumiGLO chemiluminescence reagents (Cell Signaling Technology).

Statistical Analysis

All results are expressed as mean±SEM. Statistical significance was evaluated by 1-way ANOVA followed by Fisher's analysis, Scheffe's F analysis, or Kruskal-Wallis test. A value of $P<0.05$ was considered statistically significant.

Results

Physiological and Morphological Assessment

Complete resection of the left femoral artery resulted in a similar decrease in calf blood pressure ratio among the 3 groups before the initiation of therapy (day 10) (Figure 2A). However, the calf blood pressure ratio on day 38 was highest in the AM-gelatin groups, followed by the naked AM group and subsequently the control group. The laser Doppler flow in hind limb was highest in the AM-gelatin group, followed by the naked AM group and the control group (Figure 2B). The calf blood pressure ratio and laser Doppler flow 4 weeks after gene transfer did not significantly differ between the control group and Lac Z-gelatin group. Lower hind limb necrosis was minimal in the AM-gelatin group, followed by the naked AM group and the control group (Figure 2C). Thigh muscle necrosis was also minimal in the AM-gelatin group. Similarly, the muscle weight ratio (ischemic/normal) on day 38 was highest in the AM-gelatin group (Table). Neither mean arterial pressure nor heart rate significantly differed among the 3 groups.

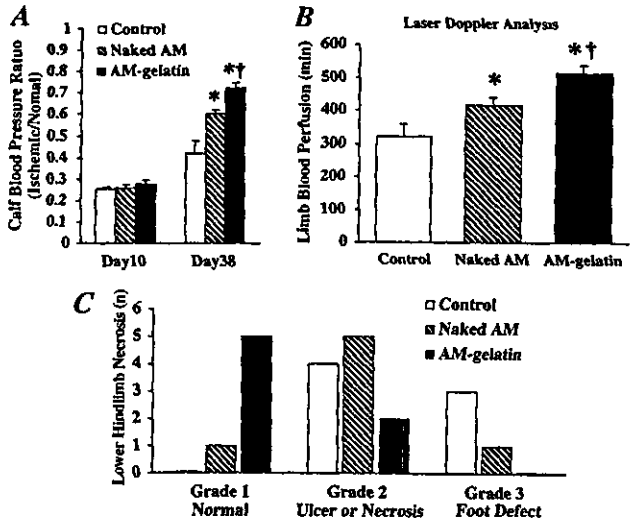

Figure 2. A, Calf blood pressure ratio (ischemic/normal hind limb) before (on day 10) and after (on day 38) gene transfer. B, Measurement of laser Doppler flow on day 38. Data are mean±SEM. *$P<0.05$ vs control group; †$P<0.05$ vs naked AM group. C, Number of cases of each grade of lower hind limb necrosis on day 38. Lower hind limb necrosis was minimal in the AM-gelatin group. Number of necrosis or foot defect is statistically significant among the 3 groups ($P<0.05$ by Kruskal-Wallis test).

Angiographic Analysis

Angiograms 4 weeks after gene transfer (day 38) showed the development of collateral arteries in the naked AM and

Physiological Characteristics

	Control	Naked AM	AM-Gelatin
No. of rabbits	7	7	7
Body weight, kg	2.46±0.06	2.65±0.10	3.16±0.09
MAP, mm Hg	112±3	114±3	116±2
HR, beats/min	269±12	253±5	262±7
Muscle weight ratio	0.71±0.03	0.84±0.02*	0.95±0.02*†

MAP indicates mean arterial pressure; HR, heart rate; and muscle weight ratio, ratio of muscle weight in ischemic hind limb to that in nonischemic hind limb. Data are mean±SEM.

*$P<0.01$ vs control group; †$P<0.05$ vs naked AM group.

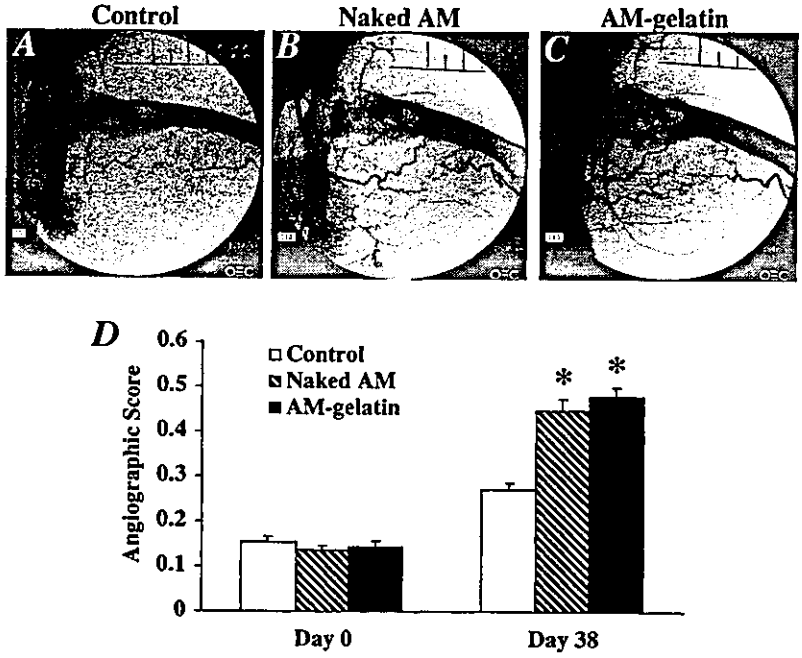

Figure 3. Representative angiograms of control group (A), naked AM group (B), and AM-gelatin group (C) on day 38. Collateral arteries were well developed in the naked AM and AM-gelatin groups. D, Angiographic score on days 0 and 38 in each group. Angiographic score on day 38 was significantly higher in the naked AM and AM-gelatin groups than in the control group. Data are mean±SEM. *$P<0.001$ versus control group.

AM-gelatin groups compared with that in the control group (Figure 3, A through C). Quantitative analysis of collateral vessels demonstrated that the angiographic score in both the naked AM and AM-gelatin groups was significantly higher than that in the control group (Figure 3D). Angiographic score did not significantly differ between the control group and Lac Z-gelatin group.

To examine the development of collateral vessels in an earlier stage, other rabbits (n=4 each) were examined 2 weeks after gene transfer (day 24). Angiograms showed significant collateral development in the naked AM and AM-gelatin groups compared with that in the control group.

Histological Examination

Alkaline phosphatase staining of ischemic hind limb muscle showed marked augmentation of neovascularization in both the naked AM and AM-gelatin groups compared with the control group (Figure 4, A through C). Quantitative analysis demonstrated that capillary density of the ischemic adductor muscle was highest in the AM-gelatin group (Figure 4D). Analysis of the capillary/muscle fiber ratio yielded similar results. Seven days after gene transfer, intense immunostaining for Ki67 was observed in vascular endothelial cells of the naked AM and the AM-gelatin groups (Figure 4, E through G).

AM Expression and Akt Phosphorylation After Gene Transfer

Seven days after gene transfer, modest immunostaining for human AM was observed in the naked AM group, whereas AM immunoreactivity was intense surrounding the gelatin in the AM-gelatin group (Figure 5, A through C). Tissue content of human AM was significantly increased both in the naked AM and the AM-gelatin groups 7 days after gene transfer (Figure 5D). The AM level in the AM-gelatin group was significantly higher that in the naked AM group. Two weeks after gene transfer, AM overexpression was observed only in the AM-gelatin group. The expression of endogenous VEGF and its receptors (Flt-1 and Flk-1) did not differ among the 3 groups (data not shown). Western blot analysis revealed that phosphorylated Akt in ischemic muscles was increased in both the naked AM and AM-gelatin groups 7 days after gene transfer (Figure 5E). Intense immunostaining for phosphory-

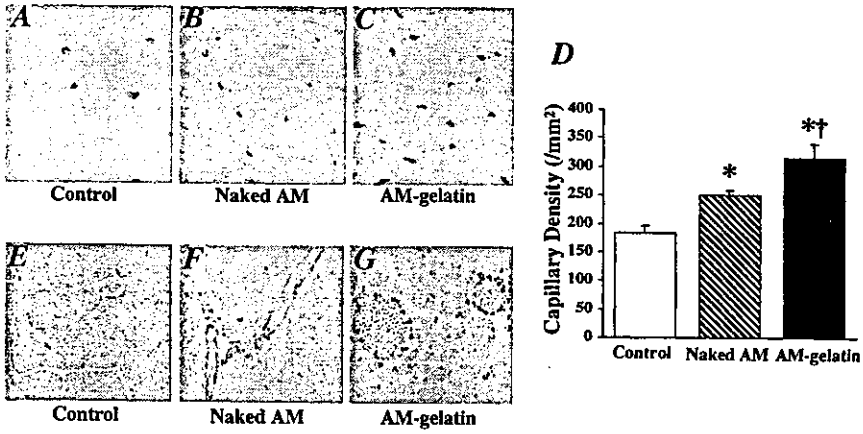

Figure 4. A through C, Representative examples of alkaline phosphatase staining in ischemic hind limb muscles. Magnification ×200. D, Quantitative analysis of capillary density in ischemic hind limb muscles. Data are mean±SEM. *$P<0.05$ vs control group; †$P<0.05$ vs naked AM group. E through G, Immunohistochemical analysis of Ki67 antigen, a marker for cell proliferation. Magnification ×400.

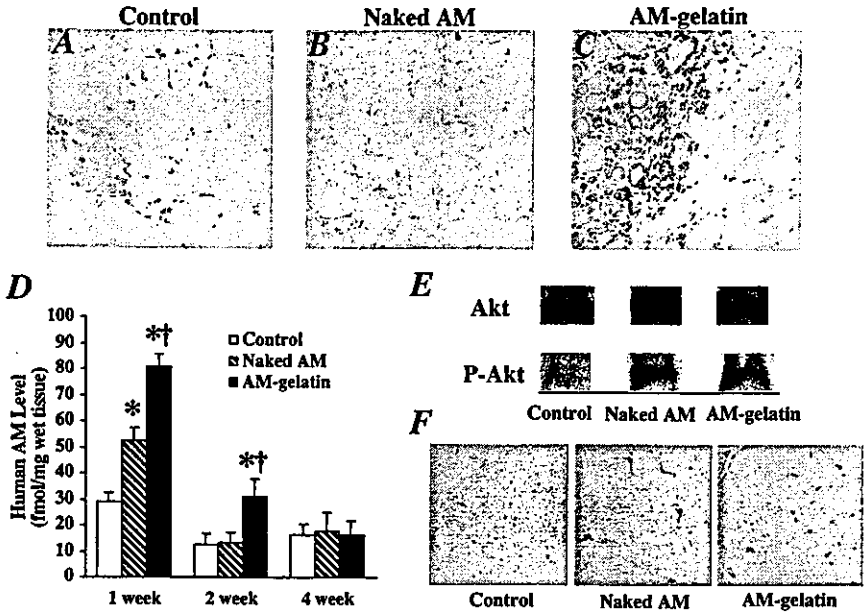

Figure 5. A through C, Immunohistochemistry for human AM 7 days after gene transfer. Intense immunostaining was observed surrounding gelatin in the AM-gelatin group. Magnification ×200. D, Time course of AM production in ischemic muscles after gene transfer. Data are mean±SEM. *$P<0.01$ vs control group; †$P<0.01$ vs naked AM group. E, Western blot analysis for Akt phosphorylation in muscles. F, Immunohistochemical staining for phosphorylated Akt 7 days after gene transfer. Phosphorylated Akt was distributed at least in endothelial cells. Magnification ×400.

lated Akt was observed at least in endothelial cells of the Naked AM and the AM-gelatin groups (Figure 5F).

Discussion

We demonstrated that (1) AM gene transfer induced hemodynamic and angiographic improvements in association with an increase in capillary density in a rabbit model of chronic hind limb ischemia. We also demonstrated that (2) administration of AM DNA-gelatin complexes markedly augmented AM expression and thereby enhanced the therapeutic effects of AM gene transfer.

AM has a variety of effects on the vasculature that include vasodilation,[1,5-7] inhibition of endothelial cell apoptosis,[8,9] and regulation of smooth muscle cell proliferation.[10] However, whether AM has angiogenic potential has remained unknown. In the present study, intramuscular administration of naked AM DNA augmented AM production in skeletal muscles, as indicated by increased tissue content and significant immunostaining of AM. As a result, AM gene transfer increased hind limb perfusion and ameliorated lower hind limb and thigh muscle necrosis in a rabbit model of hind limb ischemia. AM gene transfer may protect the ischemic hind limb partly by improving the blood flow in the ischemic hind limb because AM is originally identified as a potent vasodilating peptide.[1] Nevertheless, angiographic collateral development and high capillary density were observed in ischemic muscles after AM gene transfer. Ki67, a marker for cell proliferation, was detected in endothelial cells of microvessels after AM gene transfer. These results suggest that AM overproduction resulting from gene transfer may induce angiogenesis in a rabbit model of hind limb ischemia. Recent studies using AM gene knockout mice have shown that AM is essential for development of the vasculature during embryogenesis.[11-13] These studies support our results that AM may be an angiogenic factor. VEGF is known to induce angiogenesis and to regulate endothelial cell survival through the phosphatidylinositol 3-kinase (PI3K)/Akt pathway.[22] Thus, the PI3K/Akt pathway is considered to regulate multiple critical steps in angiogenesis, including endothelial cell survival, proliferation, migration, and capillary-like structure formation.[14] A recent study has reported that AM promotes proliferation and migration of human umbilical vein endothelial cells at least in part through the PI3K/Akt pathway.[21] The present study demonstrated that phosphorylated Akt is increased at least in endothelial cells after AM gene transfer. AM gene transfer did not influence endogenous VEGF and its receptors. Taken together, it is interesting to speculate that AM may directly induce angiogenesis through the PI3K/Akt pathway.

In the present study, we used positively charged biodegradable gelatin as a nonviral vector. We have shown that basic fibroblast growth factor (bFGF) is ionically linked with gelatin, which enhances the angiogenic effects of bFGF by delaying protein degradation.[15] Thus, biodegradable gelatin has been used as a carrier of protein. However, little information is available regarding the therapeutic potential of gelatin as a nonviral vector for gene transfer. In the present study, we demonstrated that RITC-labeled AM DNA was incorporated into positively charged gelatin. In addition, intramuscular administration of AM DNA-gelatin complexes strongly enhanced AM production compared with that of naked AM DNA. These results suggest that biodegradable gelatin may serve as a vector for gene transfer. In fact, AM DNA-gelatin complexes induced more potent angiogenic effects in a rabbit model of hind limb ischemia than naked AM DNA, as evidenced by significant increases in histological capillary density, calf blood pressure ratio, laser Doppler flow, and muscle weight ratio and a decrease in necrosis of lower hind limb and thigh muscles. These results suggest that the use of biodegradable gelatin as a nonviral vector augments AM expression and enhances AM-induced angiogenic effects. The angiogenic effects of AM-gelatin complexes were comparable to those of bFGF-gelatin complexes (data not shown). AM DNA-gelatin complexes were distributed mainly in connective tissues. We have recently demonstrated that gelatin-DNA complex is readily phagocytosed by mac-

rophages, monocytes, endothelial progenitor cells, and so on, resulting in gene expression within these phagocytes.[23,24] These findings raise the possibility that AM secreted from these cells acts on muscles in a paracrine fashion. Unlike AM production in the naked AM group, AM overexpression in the AM-gelatin group lasted for longer than 2 weeks. Thus, it is interesting to speculate that delaying gene degradation by gelatin may be responsible for the highly efficient gene transfer.

Currently, a highly efficient and safe gene delivery system is needed for gene therapy in humans. The present study demonstrated that the use of gelatin, which is considered to be less biohazardous than viral vectors, enhanced the angiogenic potential of AM DNA. Thus, gelatin-mediated AM gene transfer may be a new therapeutic strategy for the treatment of severe peripheral vascular diseases. However, the initial success of gelatin-mediated AM gene therapy reported here should be confirmed by long-term experiments, and extensive toxicity studies in animals are needed before clinical trials.

Study Limitation

First, histological capillary density, calf blood pressure ratio, and laser Doppler flow were significantly higher in the AM-gelatin group than in the naked AM group. However, the angiographic score did not significantly differ between the two. This discrepancy raises the possibility that conventional angiography may have insufficient resolution to fully visualize the angiogenic microvessels. Second, human AM level was slightly elevated in the control group. This implies that the anti-human AM antibody used in this radioimmunoassay had some cross-reactivity with endogenous rabbit AM. Nevertheless, human AM level in the muscles was highest in the AM-gelatin group within 2 weeks after gene transfer. These results suggest that AM DNA-gelatin complexes induces potent and long-lasting AM production.

Conclusions

Intramuscular administration of AM DNA induced therapeutic angiogenesis in a rabbit model of chronic hind limb ischemia. Furthermore, the use of biodegradable gelatin as a nonviral vector augmented AM expression and thereby enhanced the therapeutic effects of AM gene transfer. Thus, gelatin-mediated AM gene transfer may be a new therapeutic strategy for the treatment of peripheral vascular diseases.

Acknowledgments

This work was supported by a grant from the Japan Cardiovascular Research Foundation, HLSRG-RAMT-nano-001 and -RHGTEFB-genome-005, RGCD13C-1 from MHLW, grants from NEDO, a Grant-in-Aid for Scientific research from MECSST (13470154 and13877114), and the Promotion of Fundamental Studies in Health Science of the Organization for Pharmaceutical Safety and Research (OPSR) of Japan.

References

1. Kitamura K, Kangawa K, Kawamoto M, et al. Adrenomedullin: a novel hypotensive peptide isolated from human pheochromocytoma. *Biochem Biophys Res Commun.* 1993;192:553–560.
2. Sugo S, Minamino N, Kangawa K, et al. Endothelial cells actively synthesize and secrete adrenomedullin. *Biochem Biophys Res Commun.* 1994;201:1160–1166.
3. Sugo S, Minamino N, Shoji H, et al. Production and secretion of adrenomedullin from vascular smooth muscle cells: augmented production by tumor necrosis factor-alpha. *Biochem Biophys Res Commun.* 1994;203:719–726.
4. Kato J, Kitamura K, Kangawa K, et al. Receptors for adrenomedullin in human vascular endothelial cells. *Eur J Pharmacol.* 1995;289:383–385.
5. Shimekake Y, Nagata K, Ohta S, et al. Adrenomedullin stimulates two signal transduction pathways, cAMP accumulation and Ca^{2+} mobilization, in bovine aortic endothelial cells. *J Biol Chem.* 1995;270:4412–4417.
6. Nagaya N, Satoh T, Nishikimi T, et al. Hemodynamic, renal, and hormonal effects of adrenomedullin infusion in patients with congestive heart failure. *Circulation.* 2000;101:498–503.
7. Nishimatsu H, Suzuki E, Nagata D, et al. Adrenomedullin induces endothelium-dependent vasorelaxation via the phosphatidylinositol 3-kinase/Akt-dependent pathway in rat aorta. *Circ Res.* 2001;89:63–70.
8. Kato H, Shichiri M, Marumo F, et al. Adrenomedullin as an autocrine/paracrine apoptosis survival factor for rat endothelial cells. *Endocrinology.* 1997;138:2615–2620.
9. Sata M, Kakoki M, Nagata D, et al. Adrenomedullin and nitric oxide inhibit human endothelial cell apoptosis via a cyclic GMP-independent mechanism. *Hypertension.* 2000;36:83–88.
10. Kano H, Kohno M, Yasunari K, et al. Adrenomedullin as a novel antiproliferative factor of vascular smooth muscle cells. *J Hypertens.* 1996;14:209–213.
11. Shindo T, Kurihara Y, Nishimatsu H, et al. Vascular abnormalities and elevated blood pressure in mice lacking adrenomedullin gene. *Circulation.* 2001;104:1964–1971.
12. Caron KM, Smithies O. Extreme hydrops fetalis and cardiovascular abnormalities in mice lacking a functional adrenomedullin gene. *Proc Natl Acad Sci U S A.* 2001;98:615–619.
13. Imai Y, Shindo T, Maemura K, et al. Evidence for the physiological and pathological roles of adrenomedullin from genetic engineering in mice. *Ann N Y Acad Sci.* 2001;947:26–34.
14. Shiojima I, Walsh K. Role of Akt signaling in vascular homeostasis and angiogenesis. *Circ Res.* 2002;90:1243–1250.
15. Tabata Y, Hijikata S, Muniruzzaman M, et al. Neovascularization effect of biodegradable gelatin microspheres incorporating basic fibroblast growth factor. *J Biomater Sci Polym Ed.* 1999;10:79–94.
16. Fukunaka Y, Iwanaga K, Morimoto K, et al. Controlled release of plasmid DNA from cationized gelatin hydrogels based on hydrogel degradation. *J Control Release.* 2002;80:333–343.
17. Takeshita S, Zheng LP, Brogi E, et al. Therapeutic angiogenesis: a single intraarterial bolus of vascular endothelial growth factor augments revascularization in a rabbit ischemic hindlimb model. *J Clin Invest.* 1994;93:662–670.
18. Van Belle E, Witzenbichler B, Chen D, et al. Potentiated angiogenic effect of scatter factor/hepatocyte growth factor via induction of vascular endothelial growth factor. *Circulation.* 1998;97:381–390.
19. Ohta H, Tsuji T, Asai S, et al. A simple immunoradiometric assay for measuring the entire molecules of adrenomedullin in human plasma. *Clin Chim Acta.* 1999;287:B131–B143.
20. Nagaya N, Nishikimi T, Yoshihara F, et al. Cardiac adrenomedullin gene expression and peptide accumulation after acute myocardial infarction in rats. *Am J Physiol Regul Integr Comp Physiol.* 2000;278:R1019–R1026.
21. Miyashita K, Itoh H, Sawada N, et al. Adrenomedullin promotes proliferation and migration of cultured endothelial cells. *Hypertens Res.* 2003;26:S93–S98.
22. Jiang BH, Zheng JZ, Aoki M, et al. Phosphatidylinositol 3-kinase signaling mediates angiogenesis and expression of vascular endothelial growth factor in endothelial cells. *Proc Natl Acad Sci U S A.* 2000;97:1749–1753.
23. Tabata Y, Ikada Y. Macrophage activation through phagocytosis of muramyl dipeptide encapsulated in gelatin microspheres. *J Pharm Pharmacol.* 1987;39:698–704.
24. Nagaya N, Kangawa K, Kanda M, et al. Hybrid cell-gene therapy for pulmonary hypertension based on phagocytosing action of endothelial progenitor cells. *Circulation.* 2003;108:889–895.

Elevated Plasma Ghrelin Level in Underweight Patients with Chronic Obstructive Pulmonary Disease

Takefumi Itoh, Noritoshi Nagaya, Masanori Yoshikawa, Atsuhiko Fukuoka, Hideaki Takenaka, Yoshito Shimizu, Yoshinori Haruta, Hideo Oya, Masakazu Yamagishi, Hiroshi Hosoda, Kenji Kangawa, and Hiroshi Kimura

Department of Internal Medicine, National Cardiovascular Center, and Departments of Biochemistry and of Regenerative Medicine and Tissue Engineering, National Cardiovascular Center Research Institute, Osaka; Second Department of Internal Medicine, Nara Medical University, Nara; and Department of Respiratory Medicine, Chugoku Rousai Hospital, Hiroshima, Japan

Ghrelin, a novel growth hormone–releasing peptide, has been shown to cause a positive energy balance by reducing fat use and stimulating food intake. This study investigated whether plasma ghrelin is associated with clinical parameters in patients with chronic obstructive pulmonary disease. Plasma ghrelin was measured in 50 patients and 13 control subjects, together with anabolic and catabolic factors. Patients were divided into two groups based on body mass index: underweight patients (n = 26) or normal weight patients (n = 24). Plasma ghrelin was significantly higher in underweight patients than in normal weight patients and healthy control subjects. Circulating tumor necrosis factor-α, interleukin-6, and norepinephrine were significantly higher in underweight patients than in normal weight patients. Plasma ghrelin correlated negatively with body mass index and correlated positively with catabolic factors such as tumor necrosis factor-α and norepinephrine. In addition, plasma ghrelin correlated positively with percent predicted residual volume and residual volume-to-total lung capacity ratio. In conclusion, plasma ghrelin was elevated in underweight patients with chronic obstructive pulmonary disease, and the level was associated with a cachectic state and abnormality of pulmonary function.

Keywords: cachexia; ghrelin; hormone; pulmonary disease, chronic obstructive

Patients with chronic obstructive pulmonary disease (COPD) often show a certain degree of cachexia. Cachexia is an independent risk factor for mortality in such patients (1–3). Studies have shown that changes in endocrine hormones such as orexin and leptin have close relationships with cachexia associated with COPD (4–6). Growth hormone (GH) and its mediator, insulin-like growth factor (IGF)-I, are anabolic hormones that are essential for skeletal growth and metabolic homeostasis (7, 8). GH treatment has been shown to increase muscle mass in patients with COPD (9), although it has adverse effects including edema and abnormal glucose tolerance. These findings suggest a role of the GH/IGF-I axis in cachexia associated with COPD.

Ghrelin, a novel endogenous GH-releasing peptide, was isolated from the stomach (10). Ghrelin stimulates the secretion of GH through a mechanism independent from that of hypothalamic GH-releasing hormone. Ghrelin has been shown to cause a positive energy balance by reducing fat utilization through GH-independent mechanisms (11). In addition, both intracerebroventricular and peripheral administration of ghrelin have been shown to elicit potent, long-lasting stimulation of food intake via activation of neuropeptide Y neurons in the hypothalamic arcuate nucleus in animals (12–14). The plasma ghrelin level has been reported to be elevated in cachectic states (15, 16). However, little information is available regarding the pathophysiology of ghrelin in COPD.

Thus, the purposes of this study were to investigate (1) whether the plasma ghrelin level is elevated in patients with COPD, and (2) whether the plasma ghrelin level is related to a cachectic state and pulmonary function in patients with COPD.

METHODS

Subjects

We studied 50 patients with COPD (46 men and 4 women; mean age, 71 years; range, 41 to 83 years). COPD was diagnosed according to Global Initiative for Chronic Obstructive Lung Disease criteria. All patients were clinically stable at the time of evaluation. This study included 13 control subjects who had normal pulmonary function. The age and sex of the control subjects were similar to those of the 50 patients. The Institutional Review Board of Nara Medical University (Nara, Japan) approved this study. All subjects provided informed consent.

Patients with COPD were divided into two groups based on body mass index (BMI): underweight patients (BMI < 20, $n = 26$), or normal weight patients (BMI ≥ 20, $n = 24$). There was no significant difference in age, sex, smoking history, disease severity, or medication use between underweight and normal weight patients with COPD (Table 1). The mean smoking history was significantly higher in patients with COPD than in control subjects.

Fat-free mass (lean body mass) was measured by bioelectrical impedance analysis to investigate the relationship between plasma ghrelin and body composition in a subsample of 16 patients (underweight patients, $n = 8$; normal weight patients, $n = 8$). Lean body mass was significantly lower in underweight patients than in normal weight patients (39.3 ± 1.4 versus 46.5 ± 2.1 kg, $p < 0.05$).

Pulmonary Function Testing

Lung volumes were measured by the helium gas dilution method, and forced expiratory flow rates were measured with a mass flow anemometer (FUDAC 70; Fukuda Denshi, Tokyo, Japan). Carbon monoxide transfer factor was measured by the single-breath method. Pulmonary function values were expressed as a percentage of predicted values (17). Arterial blood gases were measured at rest with a blood gas analyzer (ABL 720; Radiometer, Brønshøj, Denmark).

Blood Sampling and Analysis

Blood samples were taken from the antecubital vein in the morning between 7:00 and 8:00 A.M. after an overnight fast. The blood was centrifuged immediately at 4°C and stored at –80°C. Plasma ghrelin was measured by radioimmunoassay as described previously (18).

Serum IGF-I was measured by radioimmunoassay (Somatomedin CII Bayer; Bayer Medical, Tokyo, Japan). Serum tumor necrosis

(Received in original form October 14, 2003; accepted in final form July 20, 2004)

Supported by the Mochida Memorial Foundation for Medical and Pharmaceutical Research and by grants from the Japan Cardiovascular Research Foundation, the New Energy and Industrial Technology Development Organization (NEDO), the Organization for Pharmaceutical Safety and Research (OPSR) of Japan (Promotion of Fundamental Studies in Health Science), and the Research Committee, Intractable Respiratory Failure, Ministry of Health, Labor, and Welfare of Japan.

Correspondence and requests for reprints should be addressed to Noritoshi Nagaya, M.D., Department of Regenerative Medicine and Tissue Engineering, National Cardiovascular Center Research Institute, 5-7-1 Fujishirodai, Suita, Osaka 565-8565, Japan. E-mail: nagayann@hsp.ncvc.go.jp

Am J Respir Crit Care Med Vol 170. pp 879–882, 2004
Originally Published in Press as DOI: 10.1164/rccm.200310-1404OC on July 21, 2004
Internet address: www.atsjournals.org

TABLE 1. PATIENT CHARACTERISTICS

	Control (n = 13)	COPD Normal Weight (n = 24)	COPD Underweight (n = 26)
Age, yr	69 ± 2	71 ± 2	71 ± 2
Sex, male/female	11/2	23/1	23/3
Body mass index, kg/m²	24.2 ± 0.7	24.2 ± 0.6	18.0 ± 0.3*,†
Smoking history, pack-years	17.6 ± 5.8	69.4 ± 6.2*	53.9 ± 5.9*
Severity stage, n			
I	NA	6	2
II	NA	5	7
III	NA	9	11
IV	NA	4	6
Medication use, n			
Anticholinergics	NA	11	16
β-Agonists	NA	15	14
Inhaled corticosteroids	NA	8	7
Xanthines	NA	14	14
Pulmonary function			
FEV_1, % predicted	93.0 ± 3.9	47.7 ± 4.4*	47.6 ± 3.5*
FEV_1/FVC, %	84.0 ± 2.3	41.4 ± 2.5*	41.7 ± 2.8*
VC, % predicted	95.7 ± 2.0	90.6 ± 5.5	84.8 ± 3.4
RV, % predicted		132.3 ± 7.8	152.0 ± 9.2
TLC, % predicted		101.2 ± 2.9	105.6 ± 3.9
RV/TLC, %		48.7 ± 2.3	52.8 ± 1.7
D_{LCO}, % predicted		61.6 ± 7.8	41.9 ± 5.5†
Pa_{O_2}, mm Hg		72.1 ± 1.7	71.4 ± 2.0
Pa_{CO_2}, mm Hg		44.5 ± 1.4	44.1 ± 1.6

Definition of abbreviations: D_{LCO} = diffusing capacity of the lung for carbon monoxide; NA = not applicable; RV = residual volume; RV/TLC, RV-to-TLC ratio; TLC = total lung capacity; VC = vital capacity.

Data represent means ± SEM.

*$p < 0.05$ versus control.

†$p < 0.05$ versus normal weight.

TABLE 2. CIRCULATING LEVELS OF HORMONAL AND BIOCHEMICAL FACTORS

	Control (n = 13)	COPD Normal Weight (n = 24)	COPD Underweight (n = 26)
Total protein, g/dl	7.5 ± 0.1	7.2 ± 0.1	7.0 ± 0.1*
Albumin, g/dl	4.6 ± 0.1	4.5 ± 0.1	4.4 ± 0.1
Total cholesterol, mg/dl	221 ± 7	206 ± 6	192 ± 5*
Triglyceride, mg/dl	119 ± 9	106 ± 11	68 ± 4†,‡
Fasting glucose, mg/dl	109 ± 6	99 ± 4	97 ± 3
Prealbumin, mg/dl	30.3 ± 1.8	27.2 ± 0.8	23.0 ± 0.7†,‡
Retinol-binding protein, g/dl	4.6 ± 0.4	3.9 ± 0.2	3.0 ± 0.1†,‡
Transferrin, mg/dl	262 ± 7	228 ± 7*	202 ± 7†,§
Tumor necrosis factor-α, pg/ml	1.4 ± 0.1	4.3 ± 0.3†	6.8 ± 0.8†,‡
Interleukin-6, pg/ml	1.6 ± 0.3	2.3 ± 0.5	4.2 ± 0.7*,§
Epinephrine, pg/ml	43 ± 8	45 ± 6	59 ± 7
Norepinephrine, pg/ml	308 ± 19	674 ± 76*	982 ± 97†,§
Insulin-like growth factor-1, ng/ml	107 ± 6	137 ± 7*	114 ± 6§
Insulin, μU/ml	8.2 ± 0.8	7.0 ± 0.8	3.9 ± 0.6†,‡
Testosterone, ng/dl	419 ± 32	421 ± 19	484 ± 24

Data represent means ± SEM.

*$p < 0.05$ versus control.

†$p < 0.01$ versus control.

‡$p < 0.01$ versus normal weight.

§$p < 0.05$ versus normal weight.

factor-α, interleukin-6, and insulin were measured by enzyme immunoassay (Quantikine HS [R&D Systems, Minneapolis, MN]; TFB kit [TFB, Tokyo, Japan]; and AIA-PACK IRI [Tosoh, Tokyo, Japan], respectively). Plasma epinephrine and norepinephrine were measured by high-performance liquid chromatography (HLC8030; Tosoh). Serum testosterone in male subjects was measured by radioimmunoassay (DPC testosterone kit; DPC, Los Angeles, CA). Serum prealbumin, retinol-binding protein, and transferrin were measured by nephelometry (Dade Behring, Deerfield, IL).

Statistical Analysis

Data are expressed as means ± SEM. Comparisons of parameters between the two groups were made by Fishes exact test or unpaired Student *t* test. Comparisons of parameters among three groups were made by one-way analysis of variance followed by the Scheffé multiple comparison test. Five groups (control subjects and patients with Stage I, II, III, and IV COPD) were compared by one-way analysis of variance followed by the Scheffé multiple comparison test. Independent relations between plasma ghrelin and pulmonary function parameters were examined by multivariate regression analyses. A p value less than 0.05 was considered statistically significant.

RESULTS

Biochemical Factors

Serum total protein and total cholesterol were significantly lower in underweight patients with COPD than in control subjects (Table 2). In addition, serum triglyceride, prealbumin, retinol-binding protein, and transferrin were significantly lower in underweight patients than in normal weight patients and control subjects.

Plasma Ghrelin and Cachectic State in Patients with COPD

The plasma ghrelin level was significantly higher in patients with COPD than in control subjects (237 ± 13 versus 157 ± 10 fmol/ml, $p < 0.01$). In particular, the plasma ghrelin level was higher in underweight patients than in normal weight patients and control subjects (272 ± 20 versus 195 ± 11 and 157 ± 10 fmol/ml, respectively, $p < 0.01$; Figure 1). The level did not significantly differ between normal weight patients and control subjects. The plasma ghrelin level correlated negatively with BMI ($r = -0.38$, $p < 0.01$; Figure 2). In addition, plasma ghrelin level correlated negatively with fat-free mass (lean body mass) ($r = -0.49$, $p < 0.05$) in a subsample of 16 patients.

Circulating levels of catabolic factors such as tumor necrosis factor-α and norepinephrine were significantly higher in both COPD groups than in control subjects (Table 2). Furthermore, the increases in these catabolic factors were marked in underweight patients compared with normal weight patients. On the other hand, circulating levels of anabolic factors such as IGF-I and insulin were significantly lower in underweight patients than in normal weight patients, although these anabolic factors in normal weight patients ware increased (IGF-I) or unchanged (insulin) compared with those in control subjects. The plasma ghrelin level correlated positively with serum tumor necrosis

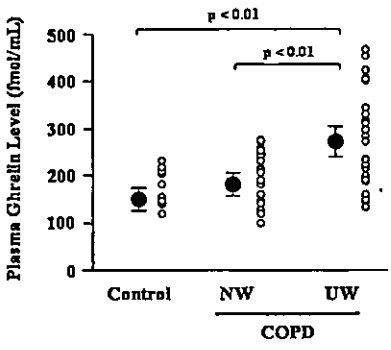

Figure 1. Plasma level of ghrelin in control subjects (Control), normal weight patients with chronic obstructive pulmonary disease (COPD) (NW), and underweight patients with COPD (UW).

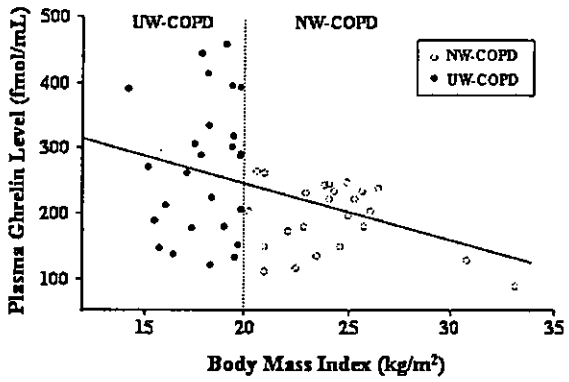

Figure 2. Correlation between plasma ghrelin level and body mass index in patients with COPD. Patients with COPD were divided into two groups: normal weight patients (NW-COPD) and underweight patients (UW-COPD). $r = -0.38$, $p < 0.01$.

factor-α ($r = 0.47$, $p < 0.01$) and plasma norepinephrine ($r = 0.40$, $p < 0.01$), but not serum IGF-I ($r = 0.12$, $p = 0.83$) and insulin ($r = -0.25$, $p = 0.27$). The plasma ghrelin level did not significantly differ between COPD patients with (n = 15) and without (n = 35) corticosteroid therapy (255 ± 27 versus 225 ± 14 fmol/ml, p = NS).

Plasma Ghrelin and Pulmonary Function in Patients with COPD

The plasma ghrelin level was higher in COPD patients with Stage IV disease than in control subjects (283 ± 31 versus 157 ± 10 fmol/ml, $p < 0.05$; Figure 3). Plasma ghrelin level tended to correlate negatively with percent predicted forced expiratory volume in one second ($r = -0.28$, $p = 0.07$), although the correlation did not reach statistical significance. Interestingly, plasma ghrelin level correlated positively with percent predicted residual volume ($r = 0.34$, $p < 0.05$) and residual volume-to-total lung capacity ratio ($r = 0.33$, $p < 0.05$) (Figure 4). Multiple regression analysis demonstrated that percent predicted residual volume or the residual volume-to-total lung capacity ratio was an independent determinant of plasma ghrelin level (each $p < 0.05$) even after adjustment for age, sex, and BMI. On the other hand, the plasma ghrelin level did not significantly correlate with any other pulmonary function parameters.

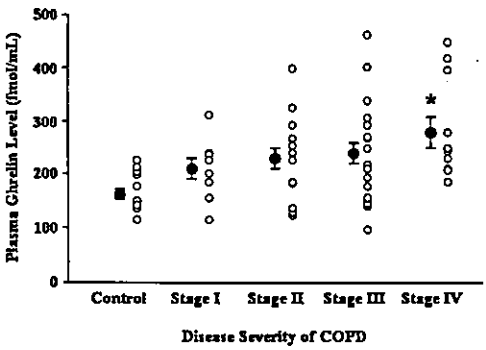

Figure 3. Plasma ghrelin level in patients with COPD according to disease severity based on Global Initiative for Chronic Obstructive Lung Disease guidelines. *$p < 0.05$ versus control.

DISCUSSION

In the present study, we demonstrated that (*1*) the plasma ghrelin level was elevated in underweight patients with COPD, and that (*2*) plasma ghrelin correlated negatively with BMI and correlated positively with circulating levels of tumor necrosis factor-α and norepinephrine. We also demonstrated that (*3*) the plasma ghrelin level was associated with indexes of hyperinflation including percent predicted residual volume and residual volume-to-total lung capacity ratio.

Ghrelin strongly stimulates GH release through a mechanism independent from that of hypothalamic GH-releasing hormone (10). Ghrelin has also been shown to cause a positive energy balance by reducing fat utilization and stimulating food intake (11–14). These findings suggest that ghrelin induces anabolic effects through GH-dependent and independent mechanisms. Thus, we investigated the pathophysiological significance of ghrelin in pulmonary cachexia. In the present study, we defined underweight as BMI < 20 kg/m². Some nutritional parameters including serum triglyceride, prealbumin, retinol-binding protein, and transferrin were also lower in underweight patients than in normal weight patients. These results suggest that "underweight" defined in the present study is accompanied by malnutrition. We demonstrated that plasma ghrelin level was higher in underweight patients than in normal weight patients. Furthermore, the plasma ghrelin level correlated negatively with BMI and lean body mass. These results suggest that the plasma ghrelin level is elevated in response to a cachectic state. Earlier studies have shown that hormonal changes and cytokine activation induce a catabolic state in patients with COPD, resulting in the development of cachexia (4–6, 19). In fact, some catabolic factors such as tumor necrosis factor-α, interleukin-6, and norepinephrine were significantly higher in underweight patients than in normal weight patients, whereas anabolic factors including IGF-I and insulin were significantly lower in underweight patients than in normal weight patients. The plasma ghrelin level correlated positively with catabolic factors such as tumor necrosis factor-α and norepinephrine. Considering the positive energy effects induced by ghrelin, increased ghrelin may represent a compensatory mechanism under catabolic–anabolic imbalance in cachectic patients with COPD. Unexpectedly, the serum IGF-I level was significantly higher in normal weight patients than in control subjects. Catabolic factors including tumor necrosis factor-α and norepinephrine were significantly higher in normal weight patients than in control subjects, although the increases were marked in underweight patients. These findings raise the possibility that increased IGF-I in normal weight patients may represent a compensatory mechanism under conditions of energy imbalance.

In the present study, the plasma ghrelin level showed significantly positive correlation with indexes of hyperinflation such as percent predicted residual volume and residual volume-to-total lung capacity ratio. In addition, the plasma ghrelin level tended to correlate negatively with percent predicted forced expiratory volume in 1 second. Thus, elevated ghrelin may be associated with abnormality of pulmonary function in patients with COPD. Because GH secretagogues receptor, a receptor for ghrelin, is expressed in the lung (20), further studies are to investigate a role of ghrelin in the lung. Although the present study demonstrated that body composition and indexes of hyperinflation were among the determinants of the plasma ghrelin level, further work will be required to determine the factors that contribute to the wide range of ghrelin levels among underweight patients with COPD.

In conclusion, the plasma ghrelin level was elevated in underweight patients with COPD, and the level was associated with a cachectic state and abnormality of pulmonary function.

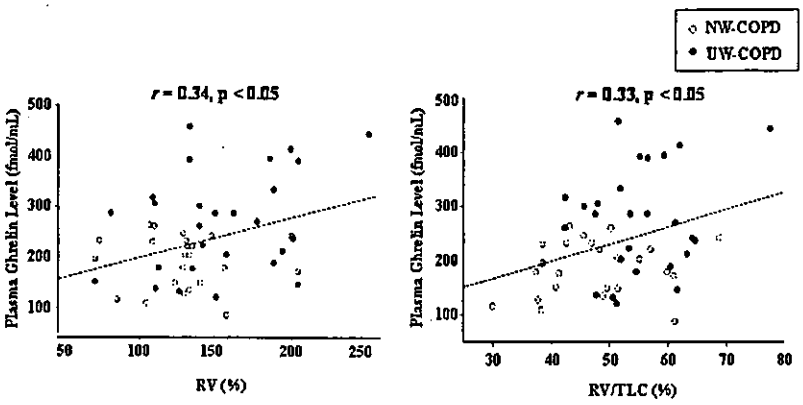

Figure 4. Correlations between plasma ghrelin level and percent predicted residual volume (RV, *left*), and between plasma ghrelin level and residual volume-to-total lung capacity ratio (RV/TLC, *right*) in patients with COPD. NW-COPD indicates normal weight patients with COPD; UW-COPD, underweight patients with COPD.

Conflict of Interest Statement: T.I. does not have a financial relationship with a commercial entity that has an interest in the subject of this manuscript; N.N. does not have a financial relationship with a commercial entity that has an interest in the subject of this manuscript; M.Y. does not have a financial relationship with a commercial entity that has an interest in the subject of this manuscript; A.F. does not have a financial relationship with a commercial entity that has an interest in the subject of this manuscript; H.T. does not have a financial relationship with a commercial entity that has an interest in the subject of this manuscript; Y.S. does not have a financial relationship with a commercial entity that has an interest in the subject of this manuscript; Y.H. does not have a financial relationship with a commercial entity that has an interest in the subject of this manuscript; H.O. does not have a financial relationship with a commercial entity that has an interest in the subject of this manuscript; M.Y. does not have a financial relationship with a commercial entity that has an interest in the subject of this manuscript; H.H. does not have a financial relationship with a commercial entity that has an interest in the subject of this manuscript; K.K. does not have a financial relationship with a commercial entity that has an interest in the subject of this manuscript; H.K. does not have a financial relationship with a commercial entity that has an interest in the subject of this manuscript.

References

1. Wilson DO, Rogers RM, Wright EC, Anthonisen NR. Body weight in chronic obstructive pulmonary disease: the National Institutes of Health Intermittent Positive Breathing Trial. *Am Rev Respir Dis* 1989; 139:1435–1438.
2. Gray-Donald K, Gibbons L, Shapiro SH, Macklem PT, Martin JG. Nutritional status and mortality in COPD. *Am J Respir Crit Care Med* 1996; 153:961–966.
3. Landbo C, Prescott E, Lange P, Vestbo J, Almdal TP. Prognostic value of nutritional status in chronic obstructive pulmonary disease. *Am J Respir Crit Care Med* 1999;160:1856–1861.
4. Takabatake N, Nakamura H, Minamihaba O, Inage M, Inoue S, Kagaya S, Yamaki M, Tomoike H. A novel pathophysiologic phenomenon in cachexic patients with chronic obstructive pulmonary disease: the relationship between the circadian rhythm of circulating leptin and the very low-frequency component of heart rate variability. *Am J Respir Crit Care Med* 2001;163:1314–1319.
5. Matsumura T, Nakayama M, Satoh H, Naito A, Kamahara K, Sekizawa K. Plasma orexin-A levels and body composition in COPD. *Chest* 2003; 123:1060–1065.
6. Debigare R, Marquis K, Cote CH, Tremblay RR, Michaud A, LeBlanc P, Maltais F. Catabolic/anabolic balance and muscle wasting in patients with COPD. *Chest* 2003;124:83–89.
7. Bark TH, McNurlan MA, Lang CH, Garlick PJ. Increased protein synthesis after acute IGF-I or insulin infusion is localized to muscle in mice. *Am J Physiol* 1998;275:E118–E123.
8. Amato G, Carella C, Fazio S, La Montagna G, Cittadini A, Sabatini D, Marciano-Mone C, Sacca L, Bellastella A. Body composition, bone metabolism, heart structure and function in growth hormone deficient adults before and after growth hormone replacement therapy at low doses. *J Clin Endocrinol Metab* 1993;77:1671–1676.
9. Burdet L, de Muralt B, Schutz Y, Pichard C, Fitting JW. Administration of growth hormone to underweight patients with chronic obstructive pulmonary disease: a prospective, randomized, controlled study. *Am J Respir Crit Care Med* 1997;156:1800–1806.
10. Kojima M, Hosoda H, Date Y, Nakazato M, Matsuo H, Kangawa K. Ghrelin is a growth-hormone releasing acylated peptide from stomach. *Nature* 1999;402:656–660.
11. Tschop M, Smiley DL, Heiman ML. Ghrelin induces adiposity in rodents. *Nature* 2000;407:908–913.
12. Wren AM, Small CJ, Ward HL, Murphy KG, Dakin CL, Taheri S, Kennedy AR, Roberts GH, Morgan DG, Ghatei MA, *et al.* The novel hypothalamic peptide ghrelin stimulates food intake and growth hormone secretion. *Endocrinology* 2000;141:4325–4328.
13. Nakazato M, Murakami N, Date Y, Kojima M, Matsuo H, Kangawa K, Matsukura S. A role for ghrelin in the central regulation of feeding. *Nature* 2001;409:194–198.
14. Shintani M, Ogawa Y, Ebihara K, Aizawa-Abe M, Miyanaga F, Takaya K, Hayashi T, Inoue G, Hosoda K, Kojima M, *et al.* Ghrelin, an endogenous growth hormone secretagogue, is a novel orexigenic peptide that antagonizes leptin action through the activation of hypothalamic neuropeptide Y/Y1 receptor pathway. *Diabetes* 2001;50:227–232.
15. Nagaya N, Uematsu M, Kojima M, Date Y, Nakazato M, Okumura H, Hosoda H, Shimizu W, Yamagishi M, Oya H, *et al.* Elevated circulating level of ghrelin in cachexia associated with chronic heart failure: relationships between ghrelin and anabolic/catabolic factors. *Circulation* 2001;23:2034–2038.
16. Shimizu Y, Nagaya N, Isobe T, Imazu M, Okumura H, Hosoda H, Kojima M, Kangawa K, Kohno N. Increased plasma ghrelin level in lung cancer cachexia. *Clin Cancer Res* 2003;9:774–778.
17. Berglund E, Birath G, Bjure J, Grimby G, Kjellmer I, Sandqvist L, Soderholm B. Spirometric studies in normal subjects. *Acta Med Scand* 1963;173:185–191.
18. Hosoda H, Kojima M, Matsuo H, Kangawa K. Ghrelin and des-acyl ghrelin: two major forms of rat ghrelin peptide in gastrointestinal tissue. *Biochem Biophys Res Commun* 2000;279:909–913.
19. Eid AA, Ionescu AA, Nixon LS, Lewis-Jenkins V, Matthews SB, Griffiths TL, Shale DJ. Inflammatory response and body composition in chronic obstructive pulmonary disease. *Am J Respir Crit Care Med* 2001;164: 1414–1418.
20. Gnanapavan S, Kola B, Bustin SA, Morris DG, McGee P, Fairclough P, Bhattacharya S, Carpenter R, Grossman AB, Korbonits M. The tissue distribution of the mRNA of ghrelin and subtypes of its receptor, GHS-R, in humans. *J Clin Endocrinol Metab* 2002;87:2988–2991.

ELSEVIER

Atherosclerosis 177 (2004) 353–360

ATHEROSCLEROSIS

www.elsevier.com/locate/atherosclerosis

Application of real-time RT-PCR to quantifying gene expression of matrix metalloproteinases and tissue inhibitors of metalloproteinases in human abdominal aortic aneurysm☆

Takeo Higashikata[a], Masakazu Yamagishi[a,*], Hiroaki Sasaki[b], Kenji Minatoya[b], Hitoshi Ogino[b], Hatsue Ishibashi-Ueda[c], Hiroyuki Hao[c], Noritoshi Nagaya[d], Hitonobu Tomoike[a], Aiji Sakamoto[e]

[a] *Division of Cardiovascular Medicine and Biotechnology, National Cardiovascular Center and Research Institute, 5-7-1 Fujishiro-dai, Suita, Osaka 565-8565, Japan*

[b] *Division of Cardiovascular Surgery, National Cardiovascular Center and Research Institute, 5-7-1 Fujishiro-dai, Suita, Osaka 565-8565, Japan*

[c] *Division of Pathology, National Cardiovascular Center and Research Institute, 5-7-1 Fujishiro-dai, Suita, Osaka 565-8565, Japan*

[d] *Division of Regenerative Medicine and Tissue Engineering, National Cardiovascular Center and Research Institute, 5-7-1 Fujishiro-dai, Suita, Osaka 565-8565, Japan*

[e] *Division of Biotechnology and Bioscience, National Cardiovascular Center and Research Institute, 5-7-1 Fujishiro-dai, Suita, Osaka 565-8565, Japan*

Received 23 October 2003; received in revised form 13 May 2004; accepted 8 July 2004
Available online 11 September 2004

Abstract

Backgound: The relative expression levels of matrix metalloproteinases (MMPs) and tissue inhibitors of metalloproteinases (TIMPs), key regulators in remodeling of extracellular matrix, are considered to play a pivotal role in the development of abdominal aortic aneurysm (AAA). However, few data exist regarding quantitative assessment of their expression in clinical settings. *Methods:* In 22 patients with AAA who underwent graft replacement, tissue samples of the AAA and non-dilated aorta were obtained. Using a real-time RT-PCR method that enabled quantitative measurement of mRNA levels in small tissue samples, we determined gene expression levels of MMPs and TIMPs relative to that of glutaraldehyde 3-phosphate dehydrogenase in each sample. *Results:* The expression levels of the MMP-1 and -3 genes were significantly augmented in AAA compared with non-dilated regions (4.48 ± 2.01 versus 0.26 ± 0.12, $P < 0.01$ and 1.89 ± 1.00 versus 5.01 ± 0.97, $P < 0.05$, respectively). Although genes for TIMP-1, -2 and -3 tended to be upregulated in AAA, relative expression levels of MMP-1 to TIMP-1, MMP-1 to TIMP-2, MMP-1 to TIMP-3, and MMP-3 to TIMP-2 were still higher in AAA than in non-dilated regions (1.12 ± 0.63 versus 0.10 ± 0.03, 4.13 ± 1.12 versus 0.43 ± 0.11, 1.61 ± 0.59 versus 0.14 ± 0.03, and 7.81 ± 1.60 versus 2.56 ± 0.76, respectively, $P < 0.05$). *Conclusion:* These results demonstrate that the present real-time RT-PCR method is reliable for the determination of mRNA levels in small samples of vascular tissue and that disproportional expression of both MMP-1 and MMP-3 relative to TIMPs relates pathologically to the evolution of AAA.

Keywords: Abdominal aortic aneurysm; Matrix metalloproteinase; Tissue inhibitor of metalloproteinase; Gene expression; Real-time RT-PCR

1. Introduction

The initiation and development of abdominal aortic aneurysm (AAA), a disease characterized by progressive degeneration of the abdominal aorta and a life-threatening prognosis, involve definite alterations of the structural components of the aortic wall, in which unregulated turnover

☆ Apart of this work was presented at the 52nd Annual Scientific Session, American College of Cardiology, in Chicago, and at the XIIIth International Symposium on Atherosclerosis in Kyoto, 2003.

* Corresponding author. Tel.: +81 6 6833 5012; fax: +81 6 6833 9865.
E-mail address: myamagi@hsp.ncvc.go.jp (M. Yamagishi).

0021-9150/$ – see front matter © 2004 Elsevier Ireland Ltd. All rights reserved.
doi:10.1016/j.atherosclerosis.2004.07.013

of the extracellular matrix is commonly demonstrated [1–4]. Matrix metalloproteinases (MMPs), which degrade extracellular structural proteins like elastin and collagen, and regulate tissue remodeling in a variety of pathophysiological conditions [5], could be implicated in the formation of AAA [6,7].

The activities of MMPs are regulated on multiple levels: transcription and translation of the inactive precursors (zymogens), posttranslational activation of zymogens by proteolysis, and interactions of mature MMPs with tissue inhibitors of metalloproteinases (TIMPs) [8]. Each of the four TIMPs known to date binds to and inactivates most of the MMPs [9], and expression of TIMP-1, -2, and -3 has been reported in aortic tissue [10–13]. Thus, the balance between MMP and TIMP expression is considered to regulate the net degeneration of extracellular matrix [14]. Carrell et al. [12] demonstrated that using competitive reverse transcription PCR (RT-PCR) method MMP-3 and TIMP-3 genes were characteristically overexpressed in AAA when compared with those in aortic occlusive tissues obtained from different patient groups. However, few data exist regarding the relative gene expression of MMPs and TIMPs in human samples of AAA, probably due to technical difficulties in measuring mRNA levels in relatively small samples of AAA and adjacent non-dilated tissue. In this study, we overcame this problem using real-time RT-PCR and analyzed gene expression levels of MMPs and TIMPs in the wall of AAA and non-dilated aorta. Tissue and cellular localization of MMPs and TIMPs was also examined by immunohistochemical staining.

2. Subjects and methods

2.1. Subjects

The protocol of this study was approved by the institutional ethical committee. Written informed consent was obtained from all 22 patients who underwent elective graft replacement for AAA (20 males and 2 females; mean age, 71.3 ± 1.6 years). None of the AAA patients suffered from clinically unstable state such as rupture before surgery. The diameter of AAA measured by computed tomography ranged from 50 to 68 mm (mean, 56 ± 19 mm). The prevalence of risk factors for AAA was as follows: hypertension in 18, hyperlipidemia in 14, smoking in 12, and diabetes mellitus in 5 out of 22 patients.

2.2. Aortic samples

During graft replacement for AAA, a strip of aortic wall that contained the dilated region and lacked mural thrombus was carefully excised. An infra-renal aortic strip without dilation was also obtained from seven patients as control. Mean wet weight of the AAA and non-dilated specimens was 297.9 and 83.2 mg, respectively. All the samples were quickly frozen in liquid nitrogen and stored at −80 °C until extraction of RNA. A part of the tissue was placed in tissue fixative (Histochoice, Hedwin, Baltimore) for immunohistochemical evaluation.

2.3. RNA preparation and cDNA synthesis

The samples were homogenized in 1.0 ml ISOGEN™ reagent (Nippon Gene, Tokyo, Japan), thoroughly mixed with 0.2 ml chloroform, and centrifuged at 15,000 × *g* for 15 min at 4 °C.

The aqueous supernatant was transferred into a micro test tube, mixed with 0.6 ml isopropanol, and centrifuged at 15,000 × *g* for 15 min at 4 °C. The precipitated total RNA was rinsed with 70% ethanol, and then resuspended in RNase-free water. The concentration and integrity of the extracted total RNA were assessed using spectrophotometry and formaldehyde/agarose gel electrophoresis. Then, 10 μg total RNA was treated with DNase Free™ reagent (Ambion, Austin, TX) for 60 min, and then reverse-transcribed with Superscript II™ (Invitrogen, Carlsbad, CA) at 37 °C for 60 min using random primers (TaKaRa, Tokyo, Japan). The volume of the resultant cDNA mixture was adjusted to 100 μl by adding double-distilled water, and stored in small aliquots at −20 °C until further use. The integrity of each cDNA mixture was checked by amplification of glutaraldehyde 3-phosphate dehydrogenase (GAPDH) (Fig. 1A) with *ExTaq* (TaKaRa, Tokyo, Japan), using the primer set 5′-ACCACAGTCCATGCCATCAC-3′/5′-TCCACCACCCTGTTGCTGTA-3′.

2.4. Primers and probes for real-time RT-PCR

Using Primer Express™ software (Applied Biosystems, Foster, CA), several sets of primers were designed for each of the genes for MMP-1, -2, -3 and -9 and TIMP-1, -2 and -3. The primer set amplifying a target cDNA most effectively, which was estimated by electrophoresis and staining with ethidium bromide, was selected for final use (Fig. 1). Subsequently, the TaqMan probe inherent to each primer set was prepared, which was an oligonucleotide labeled with a reporter dye (FAM) at the 5′-end and a quencher dye (TAMRA) at the 3′-end. The sequences of the primers and TaqMan probes used in this study are summarized in Table 1.

2.5. Real-time RT-PCR

Real-time RT-PCR was performed using an ABI PRISM 7700 Sequence Detection System (Applied Biosystems). The reaction solution was assembled in a volume of 25 μl, which comprised TaqMan Universal PCR Master Mix (Applied Biosystems), forward and reverse primers (final concentration 300 nM each), TaqMan probe (final concentration 200 nM) and cDNA mixture (25 ng). The conditions for real-time RT-PCR were preheating at 50 °C for 2 min and at 95 °C for 10 min, followed by 40 cycles of shuttle heating at 95 °C for 15 s and at 60 °C for 1 min. Throughout this study, the

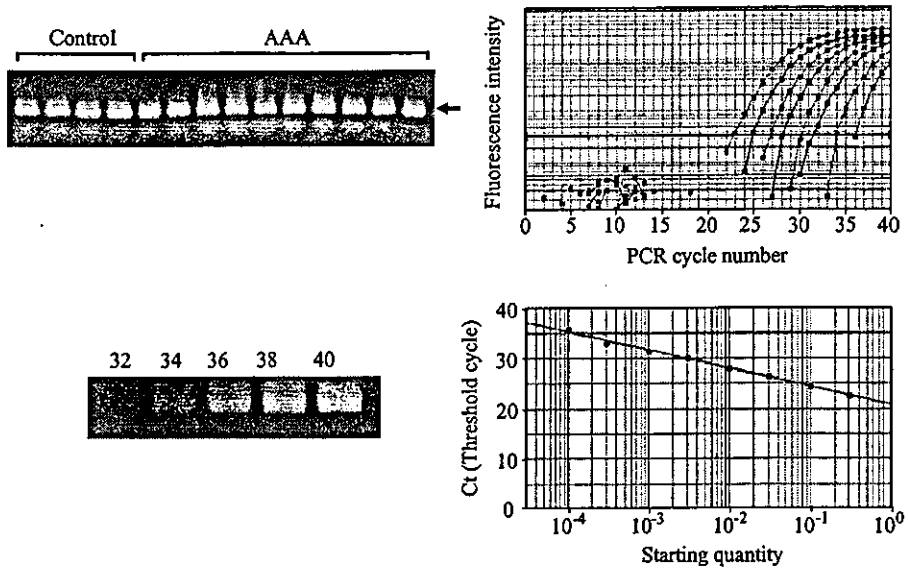

Fig. 1. Validation of cDNA synthesis and real-time RT-PCR. (Left) In electrophoretic analysis of RT-PCR for GAPDH, the amount of PCR product for GAPDH, indicated by an arrow, was equivalent among 12 representative AAA and 4 non-dilated (control) cDNAs. As for cycle-dependent amplification of MMP-1 cDNA, the numbers of cycles of PCR are shown above the electrophoretic gel. Note that the PCR product of MMP-1 was exponentially amplified according to the number of cycles. (Right) For the amplification curve of real-time RT-PCR, eight serially diluted standard cDNAs are shown. The ordinate is the logarithm of the fluorescent signal from the TaqMan probe for MMP-1 cDNA. The threshold, indicated by the horizontal line, was set at the signal intensity where the PCR products for MMP-1 exhibited exponential growth for all cDNAs. The intercept of the threshold and each amplification curve gave Ct (threshold cycle) for MMP-1 of each diluted standard cDNA. In the working standard of real-time RT-PCR for MMP-1, the abscissa is the logarithm of the dilution factor for the standard cDNA. The initial quantity of MMP-1 in a test cDNA mixture was predicted as the intercept of its Ct and this working standard.

cDNA mixture from a particular AAA sample was used to generate the working standard for quantitation of the cDNA of interest, which plots the relationship between the dilution of the standard cDNA and the corresponding Ct value (the number of cycles necessary to obtain a threshold fluorescent signal) (Fig. 1). The initial quantity of the cDNA of interest in a certain cDNA mixture was calculated from the working standard and then normalized to that of GAPDH determined with Pre-developed TaqMan Assay Reagent Endogenous Control™ (Applied Biosystems). The normalized value for each target cDNA reflects the expression level of the corresponding gene in a test sample relative to the standard tissue sample.

The methodological validity of real-time RT-PCR used in the present study was verified by comparing with the conventional RT-PCR using *ExTaq* [15]. Using cDNA mixtures of 250 ng, approximately 10 times as much as those used for real-time RT-PCR, we set up a series of RT-PCR with amplification cycles of 27, 30, 33 and 36. After acrylamide gel electrophoresis and SYBR Green staining, the target PCR products were quantified by densitometry (EDAS290, KODAK) and then plotted against PCR cycles.

2.6. Immunohistochemical study

After overnight fixation, the samples were embedded in paraffin and sectioned at 4 μm intervals. Tissue sections were deparaffinized with xylene followed by immersion in graded alcohol. They were washed three times for 5 min each in phosphate-buffered saline (PBS) and blocked with bovine serum albumin for 60 min. Specimens were then incubated with primary antibodies against CD68, MMP-1, -2, -3, -9 and TIMP-1, -2, -3 (Fuji Chemical, Tokyo, Japan) overnight at 4 °C. After they were washed in PBS, specimens were incubated with biotinylated rabbit anti-mouse IgG for 60 min at room temperature. Specimens were then washed with PBS and stained with horseradish peroxidase-conjugated streptavidin. The tissue sections were also stained with hematoxylin-eosin for histologic evaluation.

2.7. Data analysis

The mean and standard error of triplicate data are presented. Statistical analysis was performed by Mann–Whitney test using Stat View 5.0 software on a Macintosh computer. A P value less than 0.05 was considered significant.

3. Results

3.1. Quality of cDNAs and efficiency of real-time RT-PCR

Amplification of GAPDH was equivalent among all the cDNAs synthesized. Each primer set for PCR shown in Table 1 exponentially amplified its target cDNA depending

Table 1
Sequence of primer and probe

MMP-1 SENSE	5′-ACGGATACCCCAAGGACATCT-3′
MMP-1 ANTISENSE	5′-TCAGAAAGAGCATCGATATG-3′
MMP-1 TaqMan probe	5′-FAM-CAGCTCCTTTGGCTTC-CCTAGAACTGTGAA-TAMRA-3′
MMP-2 SENSE	5′-GGACAC ACTAAAGAAGATGC AGAAGT-3′
MMP-2 ANTISENSE	5′-CGCATGGTCTCGATGGTATTC-3′
MMP-2 TaqMan probe	5′-FAM-ACTGCCCCAGACAGGT-GATCTTGACC-TAMRA-3′
MMP-3 SENSE	5′-GAAATGAGGTACGAGCTG-GATACC-3′
MMP-3 ANTISENSE	5′-ATGGCTGC ATCGATTTTCCT-3′
MMP-3 TaqMan probe	5′-FAM-AGAGGCATCCACACCCTA-GGTTTCCCTC-TAMRA-3′
MMP-9 SENSE	5′-CCCGGAGTGAGTTGAACC A-3′
MMP-9 ANTISENSE	5′-GGATTTAC ATGGC ACTGCCA-3′
MMP-9 TaqMan probe	5′-FAM-ATGACATCCTGCAGT-GCCCTGAGGACTA-TAMRA-3′
TIMP-1 SENSE	5′-CTGCGGATACTTCC AC AGGTC-3′
TIMP-1 ANTISENSE	5′-GCAAGAGTCCATCCTGCAGTT-3′
TIMP-1 TaqMan probe	5′-FAM-CACAACCGCAGCGA-GGAGTTTCTCA-TAMRA-3′
TIMP-2 SENSE	5′-ATAAGCAGGCCTCCAACGC-3′
TIMP-2 ANTISENSE	5′-GAGCTGGACCAGTCGAAACC-3′
TIMP-2 TaqMan probe	5′-FAM-CTGTGGCCAACTGCAAAA AAAGCCTC-TAMRA-3′
TIMP-3 SENSE	5′-GC AGATAGACTC AAGGTGTGTGAAA-3′
TIMP-3 ANTISENSE	5′-TCCCTC ACTCTTAC ATGC AGAC A-3′
TIMP-3 TaqMan probe	5′-FAM-CCACTGCATGTCCC-AACCAGACTGTGT-TAMRA-3′

on the cycle number. Representative fluorescent curves of real-time RT-PCR for MMP-1 and the corresponding working standard are shown in Fig. 1. The working standard exhibited a linear relationship with a slope factor of −3.47 and correlation coefficient of >0.99. Similar results were obtained for the other target genes.

3.2. Expression levels of MMP and TIMP genes

Normalized values for MMP and TIMP expression in the AAA and non-dilated region are summarized in Table 2. The genes for MMP-1 and MMP-3 were significantly upregulated in AAA compared to non-dilated regions (Fig. 2). Enhanced expression of MMP-2 and MMP-9 was also observed in AAA, although it was not significant. Expression levels of TIMP-1, TIMP-2 and TIMP-3 genes also tended to be upregulated in AAA in comparison with those in non-dilated regions.

Overexpression of the MMP-1 gene was confirmed by conventional RT-PCR in which less amplification was required in AAA than in non-dilated regions to obtain the same amount of the PCR product, whereas GAPDH was equally obtained in every cycle of amplification (Fig. 3).

Table 2
MMP and TIMP levels in AAA and non-dilated aorta

mRNA	Control	AAA	*P* value
MMP-1	0.26 ± 0.12	4.48 ± 2.01	0.002
MMP-2	0.45 ± 0.12	0.76 ± 0.20	0.351
MMP-3	1.89 ± 1.00	5.01 ± 0.97	0.042
MMP-9	0.63 ± 0.31	1.69 ± 0.54	0.115
TIMP-1	2.22 ± 0.79	4.75 ± 1.52	0.302
TIMP-2	0.82 ± 0.14	1.28 ± 0.56	0.183
TIMP-3	1.66 ± 0.80	4.02 ± 1.35	0.408
MMP-1/TIMP-1	0.10 ± 0.03	1.12 ± 0.63	0.022
MMP-1/TIMP-2	0.43 ± 0.11	4.13 ± 1.12	0.009
MMP-1/TIMP-3	0.14 ± 0.03	1.61 ± 0.59	0.007
MMP-2/TIMP-1	0.29 ± 0.12	0.33 ± 0.16	0.261
MMP-2/TIMP-2	0.54 ± 0.08	0.87 ± 0.19	0.575
MMP-2/TIMP-3	0.37 ± 0.14	0.95 ± 0.45	0.855
MMP-3/TIMP-1	0.84 ± 0.12	1.80 ± 0.35	0.136
MMP-3/TIMP-2	2.56 ± 0.76	7.81 ± 1.60	0.035
MMP-3/TIMP-3	1.52 ± 0.38	2.76 ± 0.53	0.266
MMP-9/TIMP-1	0.43 ± 0.21	0.71 ± 0.22	0.611
MMP-9/TIMP-2	1.38 ± 0.59	1.72 ± 0.41	0.869
MMP-9/TIMP-3	0.65 ± 0.30	0.87 ± 0.29	0.971

Data are mean ± S.E.M.

3.3. Expression ratios of MMPs to TIMPs

All the combination ratios of four MMPs to three TIMPs examined in this study were higher in AAA than in control (Table 2). Among them, the expression ratios of four, MMP-1 to TIMP-1, MMP-1 to TIMP-2, MMP-1 to TIMP-3 and MMP-3 to TIMP-2, were significantly higher in AAA than in non-dilated regions (1.12 ± 0.63 versus 0.10 ± 0.03, 4.13 ± 1.12 versus 0.43 ± 0.11, 1.61 ± 0.59 versus 0.14 ± 0.03 and 7.81 ± 1.60 versus 2.56 ± 0.76, respectively, $P < 0.05$) (Fig. 4). It is of clinical interest to correlate the ratios of MMPs/TIMPs with the severity of AAA. However, there were no correlation between above four ratios of MMPs/TIMPs and size of AAA in the present study.

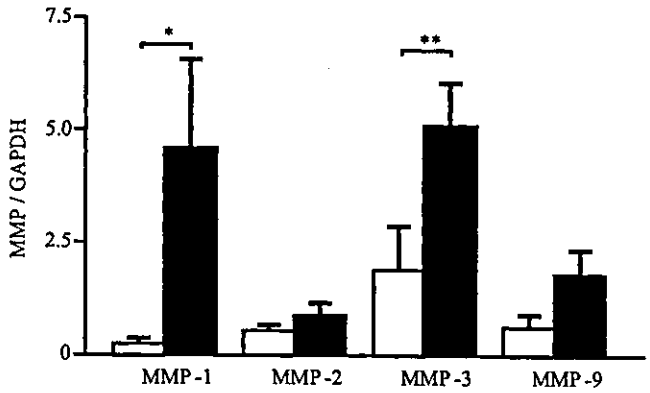

Fig. 2. Gene expression levels of MMPs in AAA and non-dilated regions. The ordinate is the relative cDNA quantity of an MMP normalized to that of GAPDH. Closed and open bars indicate AAA and non-dilated regions, respectively. Data are mean ± S.E.M. * $P < 0.01$, ** $P < 0.05$.

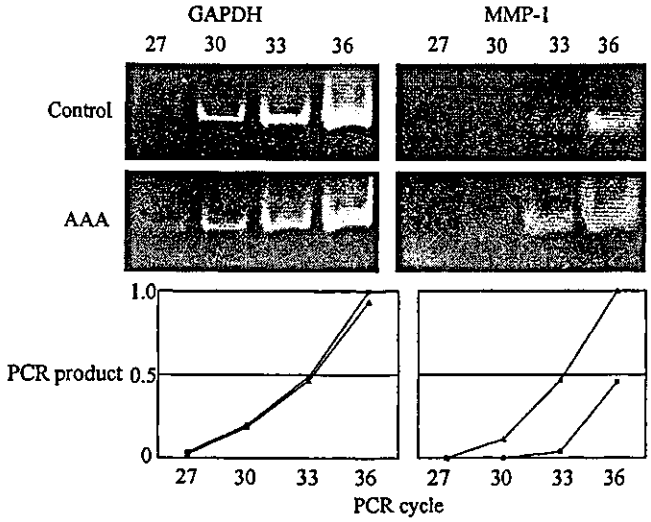

Fig. 3. Conventional RT-PCR for gene expression of GAPDH and MMP-1 in AAA and non-dilated (control) regions. (Upper) The result of gel electrophoresis and DNA staining for RT-PCR. The amplification cycles were presented above the gel. (Lower) The relationship of the amount and cycle of RT-PCR. The data for non-dilated and AAA regionas were presented in circles and triangles, respectively. In this representative case, the amounts of MMP-1 cDNAs for 30 and 33 cycles in AAA were larger than those for 33 and 36 cycles in non-dilated regions. Because PCR theoretically doubles the products through one cycle, the initial amount of cDNA for MMP-1 in this AAA was estimated to be nearly eight times as much as that in non-dilated regions, which was in good agreement with the data obtained by real time RT-PCR for the same sample with upregulation of 7.25.

3.4. Histological findings and immunochemical localization of MMPs and TIMPs

The specimens of AAA consisted of thinned or thickened vascular tissue where typical atheromatous plaques with infiltration of macrophages and lymphocytes were present. Under these conditions, macrophages in the deep layer of the intima and extracellular matrix of the lipid core were positive for MMP-1. Most macrophages were positive for MMP-3, which was also expressed in the extracellular matrix of the lipid core. There was scattered MMP-9 positivity in the macrophages and lymphocytes in the relatively deep layer. It was interesting that most macrophages positive for MMP-1 and MMP-3 were also positive for TIMP-1, which was also positive in the extracellular matrix. TIMP-2 and TIMP-3 were positive mainly in the macrophages in the intima (Fig. 5A). In the non-dilated tissue, there was mild atherosclerotic change and MMPs and TIMPs were scatteredly expressed in macrophages and/or extracelluar matrix (Fig. 5B).

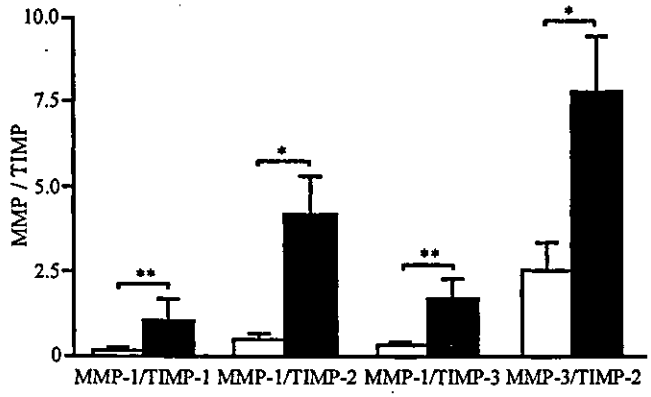

Fig. 4. Relative expression levels of MMPs versus TIMPs in AAA and non-dilated regions. The ordinate is the ratio of the normalized cDNA quantity of an MMP versus that of a TIMP. Closed and open bars indicate AAA and non-dilated regions, respectively. Data are mean ± S.E.M. * $P < 0.01$, ** $P < 0.05$.

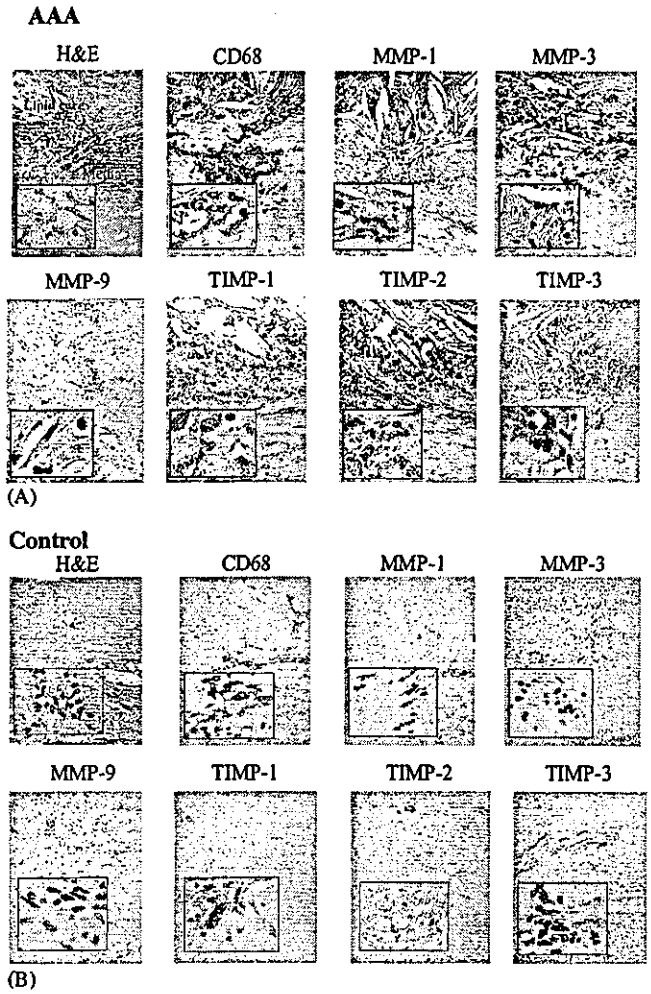

Fig. 5. Histological and immunohistochemical findings of subserial tissue sections from AAA and non-dilated (control) regions. (Upper) Hematoxylin-esosin (H & E) staining showed foam cells and lymphocytes infiltrating around the lipid core of a large atheromatous plaque (100× and 400×, original magnification). Macrophages stained by CD-68 in the deep layer of the intima and extracellular matrix of the lipid core were positive for MMP-1. Most macrophages were positive for MMP-3, which was also expressed in the extracellular matrix of the lipid core. Scattered MMP-9 positivity was observed in macrophages and lymphocytes in the deep layer of the intima. The extracellular matrix and macrophages in the intima were positive for TIMP-1. Most macrophages in the lipid core were also positive for TIMP-2 and TIMP-3. (Lower) In the non-dilated (control) region, there existed mild atherosclerotic change. Under these conditions, MMPs and TIMPs were less pronouncedly expressed in macrophages and/or extracelluar matrix than those in AAA.

4. Discussion

4.1. Methodological advantages

For detection and quantification of the mRNA of interest in AAA, we applied real-time RT-PCR method that had been already established for the quantitative evaluation of gene expression [16]. The principle of this technique is to measure the PCR product at each cycle by means of a fluorescence-labeled oligonucleotide probe, and to predict the initial amount of the cDNA of interest from Ct (the number of PCR cycles necessary to obtain the threshold signal of fluorescence). This technique makes it possible to quickly and accurately estimate the expression levels of many genes in small tissue samples from the aorta examined in the present study as well as even from the carotid and coronary artery tissues [17,18]. There are two critical parameters; the integrity of the cDNA synthesized and the amplification efficiency of the primers used for PCR. In the present study, these two parameters were assessed by conventional electrophoresis with ethidium bromide staining. The amount of PCR product for GAPDH, a representative housekeeping gene, was equivalent in all the samples, and each primer set for PCR exponentially amplified the target cDNA depending on the number of cycles. Therefore, ideal working standards could be generated for all the genes examined. In addition, real-time RT-PCR seems to have the higher sensitivity and equivalent quantitativeness as compared with conventional RT-PCR that requires the larger amount of cDNA for determination than that for the present method.

4.2. Dominant expression of MMPs over TIMPs in AAA

We showed that the gene expression of MMP-1 and MMP-3 was significantly augmented in AAA compared with that in non-dilated control regions. Although upregulation of either MMP-1 or MMP-3 in AAA was shown in different clinical studies [12,19], it is quite interesting that in the present study both MMP-1 and MMP-3 were demonstrated to be upregulated simultaneously in AAA. Carrell et al. [12] showed that expression of MMP-3 gene had highly significant increase in AAA over aortic occlusive tissues, although that of MMP-1 was not different between them. This may be explained by the possibility that MMP-1 gene was upregulated in aortic occlusive tissue [18] as well as that in AAA tissue, obscuring overexpression of MMP-1 in AAA.

MMP-1 specifically cleaves collagen types I, II, and III; which are key components of the extracellular framework of the arterial wall and major constituents of human atherosclerotic lesions and activate other MMPs such as MMP-2 and -9 [8] that degrade denatured collagen and elastin. MMP-3 digests collagen and several other extracellular matrix proteins. It also plays a crucial role in the pericellular MMP activation cascade by cleaving other MMP proenzymes such as MMP-1 and MMP-9 to their active form. Indeed, aneurysm formation in the thoracic and abdominal aorta was less frequent in mice with double knockout of the apoE and MMP-3 genes than in apoE knockout mice [20]. Thus, it is reasonable to consider that simultaneous upregulation of both MMP-1 and MMP-3 could have resulted in aggravation of AAA in the present cases. Tung et al. [21], however, conducted a gene expression survey in AAA using a cDNA macroarray technique, which failed to detect MMP-1 and MMP-3 transcript in either AAA or normal aorta. This apparent inconsistency with our and others' [12,18] results may be due to the sensitivity of signal detection with the cDNA macroarray, which is much lower than that with RT-PCR methods.

In a mouse model, elastase-induced aneurysmal degeneration of the abdominal aorta was suppressed by targeted gene disruption of MMP-9 [22]. Recently, administration of doxycycline, which mainly decreased MMP-9 [23] as well as MMP-1 [24] production, was shown to effectively prevent the formation of angiotensin II-induced AAA, providing indirect evidence for a role of MMP-9 and/or MMP-1 in AAA [25]. We observed 2.7-fold higher gene expression of MMP-9 in AAA compared with non-dilated regions, though this was not significant. Therefore, one might speculate that, in addition to MMP-1 and MMP-3, MMP-9 could be involved in the pathogenesis of AAA, although MMP-9 appears to have a protective role limiting atherosclerotic development [26].

TIMP-1, TIMP-2 and TIMP-3 all exhibited relatively higher expression in AAA than in non-dilated regions, although Carrell et al. [12] indicated that only TIMP-3 gene expression in AAA was significantly higher than that in aortic occlusive tissue. As observed in carotid occlusive tissue [18], TIMP-1 and -2 genes could be upregulated in aortic occlusive tissue which was used for comparison, obscuring the difference in expression of these genes in AAA and aortic occlusive tissues. TIMPs, which are produced by various types of cells including macrophages as observed in the present study, counteract most of the MMPs [9]. TIMPs can interfere with the proteolytic processing of MMP zymogens, as well as block substrate binding to activated MMPs which can perform their biological function after activation, and where local stoichiometric excess over endogenous inhibitors such as TIMPs prevails [27].

In a rat model in which decellularized segments of guinea pig aorta were orthotopically grafted into the abdominal aorta, aneurysmal formation of the grafted aorta was suppressed by TIMP-1 overexpression resulting from seeding of rat smooth muscle cells retrovirally transfected with the TIMP-1 gene [28]. Aneurysm formation in the thoracic and abdominal aorta was more frequent in mice with double knockout of the apoE and TIMP-1 genes than in apoE knockout mice [29]. Taken together, TIMPs seem to exert some inhibitory roles in the development of human AAA.

From this point of view, the most important finding of this study was that all the expression ratios of MMPs versus TIMPs were higher in AAA than in non-dilated regions. Particularly, the expression ratios of MMP-1/TIMPs and MMP-

3/TIMP-2, all of which were expressed in the extracellular matrix as well as in macrophages as also demonstrated by Newman et al. [30], were significantly higher in AAA. Augmentation of TIMP gene expression is considered to be an adaptive phenomenon to cope with rampant destruction of extracellular matrix by MMPs. The dominant expression of MMPs over TIMPs in AAA suggests that compensatory expression of TIMPs is insufficient to counteract the degenerative role of MMPs in the formation of AAA.

4.3. Implications and limitations

Inactivation of MMPs by pharmacological agents [25] or gene-targeting techniques [20] has been shown to effectively inhibit the development and progression of experimental AAA. The results of prolonged administration of doxycycline, a non-selective MMP antagonist, in patients with a small AAA suggested that doxycycline might have effects on AAA expansion through suppression of multiple MMPs [31]. In addition, several factors have been identified as positive regulators of the expression of TIMP genes, such as growth factors, phorbol esters and inflammatory cytokines [9]. Therefore, the effective manipulation to regulate the altered MMP/TIMP ratios as shown in the present study may further result in improving the clinical prognosis of AAA.

Although there was no correlation between MMPs/TIMPs and severity of AAA such as diameter, it is possible that velocity of aneurysm growth or changes in morphology associated with rupture may reflect different MMPs/TIMPs relationship. Examination of unstable patients in whom rapid changes in AAA diameter and/or presence of impending rupture can be monitored before surgery may clarify this issue.

One of the limitations of the present study was that as a control we used adjacent non-dilated tissue which might contain mild atherosclerotic lesions, because it was difficult to obtain normal aortic tissues from patients with AAA. It is interesting, however, to consider that the present study demonstrates the different gene expression of MMPs and TIMPs in AAA and adjacent tissue which may represent the pathophysiological condition of pre-aneurysmal aortic tissue.

In the present study, we used real-time RT-PCR, which gives an estimate of mRNA expression for each enzyme and inhibitor, and did not determine the enzyme activities. It may still be difficult, however, to extract these proteinases bound strongly to connective tissue and to quantitatively assay enzyme activities [32]. Therefore, evaluation of mRNA expression of MMPs and TIMPs by the present real-time RT-PCR method should be reliable for evaluation of the relative production of MMPs and TIMPs in clinical tissue samples. Further investigation of the regulatory mechanism of MMP and TIMP genes in which physiological and pathological stimulation upregulates an everbroader spectrum of MMPs [33] and other factors such as inflammatory cytokines [34] will provide a clue to the pathogenesis and to devising novel therapeutic agents for AAA, even at an established stage.

Acknowledgments

This work was supported in part by grants from the Ministry of Health and Welfare of Japan (to M.Y.), the Promotion of Fundamental Studies in Health Science of the Organization for Pharmaceutical Safety and Research (OPSR) of Japan (to A.S.), and the Japan Cardiovascular Research Foundation (to A.S.).

References

[1] Thompson RW. Basic science of abdominal aortic aneurysm: emerging therapeutic strategies for an unresolved clinical problem. Curr Opin Cardiol 1996;11:504–18.
[2] White JV, Haas K, Phillips S, Comerota AJ. Adventitial elastolysis is a primary event in aneurysm formation. J Vasc Surg 1993;17:371–80.
[3] Dobrin PB, Mrkvicka R. Failure of elastin or collagen as possible critical connective tissue alterations underlying aneurysmal dilatation. Cardiovasc Surg 1994;2:484–8.
[4] Satta J, Haukipuro K, Kairaluoma MI, Juvonen T. Aminoterminal propeptide of type III procollagen in the follow-up of patients with abdominal aortic aneurysms. J Vasc Surg 1997;25:909–15.
[5] Nagase H, Woessner JF. Matrix metalloproteinases. J Biol Chem 1999;274:21491–4.
[6] Thompson RW, Parks WC. Role of matrix metalloproteinases in abdominal aortic aneurysms. Ann NY Acad Sci 1996;800:157–74.
[7] Newman KM, Malon AM, Shin RD, Scholes JV, Ramey WG, Tilson MD. Matrix metalloproteinases in abdominal aortic aneurysm: characterization, purification, and their possible sources. Connect Tissue Res 1994;30:265–76.
[8] Nagase H. Activation mechanisms of matrix metalloproteinases. Biol Chem 1997;378:151–60.
[9] Brew K, Dinakarpandian D, Nagase H. Tissue inhibitors of metalloproteinases: evolution, structure and function. Biochim Biophys Acta 2000;1477:267–83.
[10] McMillan WD, Patterson BK, Keen RR, Shively VP, Cipollone M, Pearce WH. In situ localization and quantification of mRNA for 92-kDa type IV collagenase and its inhibitor in aneurysmal, occlusive, and normal aorta. Arterioscler Thromb Vasc Biol 1995;15:1139–44.
[11] McMillan WD, Patterson BK, Keen RR, Pearce WH. In situ localization and quantification of seventy-two-kilodalton type IV collagenase in aneurysmal, occlusive, and normal aorta. J Vasc Surg 1995;22:295–305.
[12] Carrell TW, Burnand KG, Wells GM, Clements JM, Smith A. Stromelysin-1 (matrix metalloproteinase-3) and tissue inhibitor of metalloproteinase-3 are overexpressed in the wall of abdominal aortic aneurysm. Circulation 2002;105:477–82.
[13] Armstrong PJ, Johanning JM, Calton Jr WC, et al. Differential gene expression in human abdominal aorta: aneurysmal versus occlusive disease. J Vasc Surg 2002;35:346–55.
[14] Sternlicht MD, Werb Z. How matrix metalloproteinases regulate cell behavior. Annu Rev Cell Dev Biol 2001;17:463–516.
[15] Sakamoto A, Ono K, Abe M, et al. Both hypertrophic and dilated cardiomyopathies are caused by mutation of the same gene, sarcoglycan, in hamster: an experimental model of disrupted dystrophin-associated glycoprotein complex. Proc Natl Acad Sci USA 1997;94:13873–8.
[16] Heid CA, Stevens J, Livak KJ, et al. Real time quantitative PCR. Genome Res 1996;6:986–94.
[17] Higo S, Nanto S, Higashikata T, et al. Impact of altered expression balance of matrix metalloproteinases and tissue inhibitor of metalloproteinases genes on coronary plaque rupture: results from quantitative tissue analysis using real-time reverse transcriptase-polymerase

chain reaction method (abstr). J Am Coll Cardiol 2004;43(suppl A):257A.
[18] Higashikata T, Yamagishi M, Ishibashi-Ueda H, et al. Impact of altered expression balance of matrix metalloproteinases and tissue inhibitor of metalloproteinases on carotid plaque rupture: results from quantitative tissue analysis using real-time RT-PCR method (abstr). Circulation 2003;108(suppl IV):IV-348.
[19] Tamarina NA, McMillan WD, Shively VP, Pearce WH. Expression of matrix metalloproteinases and their inhibitors in aneurysms and normal aorta. Surgery 1997;122:264–71.
[20] Silence J, Lupu F, Collen D, Lijnen HR. Persistence of atherosclerotic plaque but reduced aneurysm formation in mice with stomelysin-1 (MMP-3) gene inactivation. Arterioscler Thromb Vasc Biol 2001;21:1440–5.
[21] Tung WS, Lee JK, Thompson RW. Simultaneous analysis of 1176 gene products in normal human aorta and abdominal aortic aneurysms using a membrane-based complementary DNA expression array. J Vasc Surg 2001;34:143–50.
[22] Pyo R, Lee JK, Shipley JM, et al. Targeted gene disruption of matrix metalloproteinase-9 (gelatinase B) suppresses development of experimental abdominal aortic aneurysms. J Clin Invest 2000;105:1641–9.
[23] Curci JA, Mao D, Bohner DG, et al. Preoperative treatment with doxycycline reduces aortic wall expression and activation of matrix metalloproteinases in patients with abdominal aortic aneuryms. J Vasc Surg 2000;31:325–42.
[24] Axisa B, Loftus IM, Naylor AR, et al. Prospective, randomized, double-blind trial investigating the effect of doxycycline on matrix metalloproteinase expression within atherosclerotic carotid plaques. Stroke 2002;33:2858–64.
[25] Manning MW, Cassis LA, Daugherty A. Differential effects of doxycycline, a broad-spectrum matrix metalloproteinase inhibitor, on angiotensin II-induced atherosclerosis and abdominal aortic aneurysms. Arterioscler Thromb Vasc Biol 2003;23:483–8.
[26] Johnson J, George S, Newby A, Jackson C. Matrix metalloproteinases-9 and -12 have opposite effects on atherosclerotic plaque stability (abstr). Atherosclerosis 2003;4(suppl):196.
[27] Stetler-Stevenson WG, Liotta LA, Kleiner DE. Extracellular matrix 6: role of matrix metalloproteinases in tumor invasion and metastasis. FASEB J 1993;7:1434–41.
[28] Allaire E, Forough R, Clowes M, Starcher B, Clowes AW. Local overexpression of TIMP-1 prevents aortic aneurysm degeneration and rupture in a rat model. J Clin Invest 1998;102:1413–20.
[29] Silence J, Collen D, Lijnen HR. Reduced atherosclerotic plaque but enhanced aneurysm formation in mice with inactivation of the tissue inhibitor in metalloproteinase-1 (TIMP-1) gene. Circ Res 2002;90:897–903.
[30] Newman KM, Jean-Claude J, Li H, et al. Cellular localization of matrix metalloproteinases in the abdominal aortic aneurysm wall. J Vasc Surg 1994;20:814–20.
[31] Baxter BT, Pearce WH, Waltke EA, Littooy FN, Hallett JW, Kent KC, Upchurch GR, Chaikof EL, Mills JL, Fleckten B, Longo GM, Lee JK, Thompson RW. Prolonged administration of doxycycline in patients with small asymptomatic abdominal aortic aneurysms: report of prospective (phase II) multicenter study. J Vasc Surg 2002;36:1–12.
[32] Woessner JR. Quantification of matrix metalloproteinases in tissue samples. Methods Enzymol 1995;248:510–28.
[33] Chase AJ, Newby AC. Regulation of matrix metalloproteinase (Matrixin) genes in blood vessels: a multi-step recruitment model for pathological remodeling. J Vasc Res 2003;40:329–43.
[34] Higashikata T, Yamagishi M, Sasaki H, et al. Sustained upregulation of inflammatory cytokine and its receptor genes associated with proteinase activation in abdominal aortic aneurysm: results from combined study with cDNA array and real-time reverse transcriptase polymerase chain reaction methods (abstr). J Am Coll Cardiol 2004;43(suppl A):13A.

Diagnostic value of epinephrine test for genotyping LQT1, LQT2, and LQT3 forms of congenital long QT syndrome

Wataru Shimizu, MD, PhD,[a,b] Takashi Noda, MD, PhD,[a] Hiroshi Takaki, MD,[c] Noritoshi Nagaya, MD, PhD,[a] Kazuhiro Satomi, MD,[a] Takashi Kurita, MD, PhD,[a] Kazuhiro Suyama, MD, PhD,[a] Naohiko Aihara, MD,[a] Kenji Sunagawa, MD, PhD,[c] Shigeyuki Echigo, MD,[d] Yoshihiro Miyamoto, MD, PhD,[b] Yasunao Yoshimasa, MD, PhD,[b] Kazufumi Nakamura, MD, PhD,[e] Tohru Ohe, MD, PhD,[e] Jeffrey A. Towbin, MD,[f] Silvia G. Priori, MD, PhD,[g] Shiro Kamakura, MD, PhD[a]

[a]From the Division of Cardiology, Department of Internal Medicine, National Cardiovascular Center, Suita, Japan,
[b]Laboratory of Molecular Genetics, National Cardiovascular Center, Suita, Japan,
[c]Department of Cardiovascular Dynamics, National Cardiovascular Center, Suita, Japan,
[d]Department of Pediatrics, National Cardiovascular Center, Suita, Japan,
[e]Department of Cardiovascular Medicine, Okayama University Graduate School of Medicine and Dentistry, Okayama, Japan,
[f]Department of Pediatrics (Cardiology), Molecular & Human Genetics, Baylor College of Medicine, Houston, Texas, and
[g]Molecular Cardiology, Salvatore Maugeri Foundation, IRCCS, Pavia, Italy.

OBJECTIVES The aim of this study was to test the hypothesis that epinephrine test may have diagnostic value for genotyping LQT1, LQT2, and LQT3 forms of congenital long QT syndrome (LQTS).

BACKGROUND A differential response of dynamic QT interval to epinephrine infusion between LQT1, LQT2, and LQT3 syndromes has been reported, indicating the potential diagnostic value of the epinephrine test for genotyping the three forms.

METHODS The responses of 12-lead ECG parameters to epinephrine were retrospectively examined in 15 LQT1, 10 LQT2, 8 LQT3, and 10 healthy volunteers to select the best ECG criteria for separating the four groups. The epinephrine test then was prospectively conducted in 42 probands clinically affected with LQTS, their 67 family members, and 10 new volunteers. The best criteria were applied in a blinded fashion to prospectively separate a different group of 31 LQT1, 23 LQT2, 6 LQT3, and 30 Control patients (10 genotype-negative LQT1, 10 genotype-negative LQT2 family members, and 10 volunteers).

RESULTS The sensitivity (penetrance) by ECG diagnostic criteria was lower in LQT1 (68%) than in LQT2 (83%) or LQT3 (83%) before epinephrine and was improved with steady-state epinephrine in LQT1 (87%) and LQT2 (91%) but not in LQT3 (83%), without the expense of specificity (100%). The sensitivity and specificity to differentiate LQT1 from LQT2 were 97% and 96%, those from LQT3 were 97% and 100%, and those from Control were 97% and 100%, respectively, when Δ mean corrected Q-Tend ≥35ms at steady state was used. The sensitivity and specificity to differentiate LQT2 from LQT3 or Control were 100% and 100%, respectively, when Δ mean corrected Q-Tend ≥80ms at peak was used.

CONCLUSIONS Epinephrine infusion is a powerful test to predict the genotype of LQT1, LQT2, and LQT3 syndromes as well as to improve the clinical diagnosis of genotype-positive patients, especially those with LQT1 syndrome.

KEYWORDS Arrhythmia; Diagnosis; Long QT syndrome; Catecholamines; Genes

1547-5271/$ -see front matter © 2004 Heart Rhythm Society. All rights reserved.
doi:10.1016/j.hrthm.2004.04.021

Heart Rhythm (2004) 3, 276–283

Table 1 Clinical characteristics of LQT1, LQT2, LQT3, and control groups in prospective study

	LQT1 (n = 31)	LQT2 (n = 23)	LQT3 (n = 6)	Control (n = 30)
Age [yr (range)]	21 ± 14 (4–55)	27 ± 16 (6–61)	21 ± 16 (7–43)	29 ± 15 (6–64)
Age <15 yr	16/31 (52%)	7/23 (30%)	3/6 (50%)	5/30 (17%)
Female sex	17/31 (55%)	16/23 (70%)	3/6 (50%)	16/30 (53%)
Baseline heart rate (beats/min)	67 ± 9	66 ± 12	60 ± 10	72 ± 13
Peak heart rate with Epi (beats/min)	99 ± 14	96 ± 16	95 ± 10	99 ± 13
Steady-state heart rate with Epi (beats/min)	85 ± 12	76 ± 14	70 ± 12	79 ± 13
Baseline QTc interval (ms)	470 ± 41†	503 ± 33*	506 ± 41*	408 ± 19
Syncope or aborted cardiac arrest	14/31 (45%)	12/23 (52%)	2/6 (33%)	(0%)
Beta-blockers	(0%)	(0%)	(0%)	(0%)

Values are given as mean ± SD where indicated. Epi = epinephrine; QTc = corrected QT.
*$P < 0.05$ vs LQT1 and control.
†$P < 0.05$ vs control.

The congenital long QT syndrome (LQTS) is a hereditary disorder caused by mutations in genes of the potassium and sodium channels or membrane adapter located on chromosomes 3, 4, 7, 11, 17, and 21.[1–4] Among the LQT1, LQT2, and LQT3 forms, which account for approximately two thirds of genotyped patients, cardiac events are more often associated with sympathetic stimulation (physical or emotional stress) in LQT1 than in either LQT2 or LQT3 syndrome.[5–8] Concordant with the influence of sympathetic stimulation, beta-blockers are the most effective in LQT1 syndrome.[9,10] Therefore, genotyping of LQTS is of major importance because it would be helpful in managing and treating patients more effectively.[11] Preliminary studies by our and other groups have demonstrated the differential response of dynamic QT interval to epinephrine infusion between LQT1, LQT2, and LQT3 syndromes,[12,13] indicating the potential diagnostic value of the epinephrine test for genotyping the three forms. The present study was designed to test this hypothesis.

Methods

Study design and population

First, we retrospectively analyzed the response of ECG parameters to epinephrine infusion in 15 LQT1 patients (5 families), 10 LQT2 patients (5 families), 8 LQT3 patients (2 families), and 10 healthy volunteers (Control), some of whom were included in our previous study.[12] The best ECG criteria separating LQT1, LQT2, LQT3, and Control patients were selected. Then, we prospectively conducted an epinephrine test in 42 probands who were clinically diagnosed as having congenital LQTS, their 67 family members, and 10 new healthy volunteers. The best ECG criteria with the epinephrine test derived from the retrospective study were applied in a blinded fashion to differentiate LQT1, LQT2, LQT3, and Control groups in a total of 119 subjects. Molecular screening, which was performed after the epinephrine test, identified 31 genotype-positive LQT1 patients (12 families), 23 genotype-positive LQT2 patients (12 families), 6 genotype-positive LQT3 patients (3 families), 10 genotype-negative LQT1 patients (9 families), and 10 genotype-negative LQT2 patients (4 families). The study population of the prospective study included the 31 LQT1, 23 LQT2, and 6 LQT3 patients. The data from the 10 genotype-negative LQT1 patients, 10 genotype-negative LQT2 patients, and 10 healthy volunteers were pooled and referred to as Control group, because there were no significant differences in the clinical and ECG characteristics among the three groups. In the remaining 29 patients including 15 probands (15 families), no responsible mutations were identified in any LQTS genes. There were no significant differences among LQT1, LQT2, LQT3, and Control groups with regard to age, percentage of age <15 years old, gender, baseline heart rate, and peak and steady-state heart rate with epinephrine in the prospective study (Table 1). Percentage of syncope or aborted cardiac arrest was no different among LQT1, LQT2, and LQT3 groups (Table 1). The baseline corrected QT intervals in LQT2 and LQT3 groups were significantly longer than that in the LQT1 group; those in the LQT1, LQT2, and LQT3 groups were all significantly longer than that in the Control group (Table 1). Genotyping of LQTS was reviewed and approved by our Ethical Review Committee, and written informed consent was obtained from all patients or their parents when the patients were younger than 20 years. All epinephrine tests were conducted in the National Cardiovascular Center as part of a clinical

Dr. Shimizu was supported in part by the Japanese Cardiovascular Research Foundation, Vehicle Racing Commemorative Foundation, and Health Sciences Research Grants from the Ministry of Health, Labour and Welfare, and Research Grant for Cardiovascular Diseases (15C-6) from the Ministry of Health, Labour and Welfare, Japan. Dr. Priori was supported by an educational grant from the Leducq Foundation. Dr. Towbin was supported by grants from the National Institutes of Health (NIH), National Heart, Lung & Blood Institute (NHLBI) (R01 HL33843 and R01 HL51618).

Address reprint requests and correspondence: Dr. Wataru Shimizu, Division of Cardiology, Department of Internal Medicine, National Cardiovascular Center, 5-7-1 Fujishiro-dai, Suita, Osaka, 565-8565 Japan.

E-mail address: wshimizu@hsp.ncvc.go.jp.

(Received January 30, 2004; accepted April 14, 2004.)

evaluation of LQTS patients. We previously reported that the oral beta-blocker propranolol (0.5–2 mg/kg) completely suppressed the effects of epinephrine on repolarization parameters[14]; therefore, no subjects took beta-blockers at the time of the epinephrine test in either the retrospective or prospective study. Among a total of 93 genotyped LQTS patients in the retrospective and prospective studies, 85 patients were transferred to our hospital for initial evaluation of LQTS without any medications including beta-blockers, and the epinephrine test could be conducted in the absence of beta-blockers. Appropriate therapies, including beta-blockers, were started after the evaluation of LQTS. In the remaining 8 patients (3 LQT1 and 5 LQT2), beta-blockers were withheld during the evaluation of LQTS, including the epinephrine test, and then reinstated.

Clinical diagnosis

LQTS-affected individuals were diagnosed based on the ECG criteria of Keating et al,[15] including a corrected QT ≥470 ms in asymptomatic individuals and a corrected QT >440 ms for males and >460 ms for females associated with ≥1 of the following: (1) stress-related syncope, (2) documented torsades de pointes, or (3) family history of early sudden cardiac death. The LQTS score was calculated using the diagnostic criteria of Schwartz et al.[16]

Recording of standard 12-lead ECG

A standard 12-lead ECG was recorded using an FDX6521 (Fukuda Denshi Co., Tokyo, Japan) with the patient in the supine position. These ECG data were digitized using analog-to-digital converters at a sampling rate of 1,000 samples per second per channel.

Measurements

Measurement of the ECG parameters was performed against five averaged QRS complexes by an off-line computer with an analysis program developed by our institution. Q-Tend was defined as the interval between QRS onset and the point at which an isoelectric line intersected a tangential line drawn at the minimum dV/dt point of a positive T wave or at the maximum dV/dt point of a negative T wave. When a bifurcated or secondary T wave (pathologic U wave) appeared, it was included as part of the measurement of the Q-Tend, but a normal U wave, which was apparently separated from a T wave, was not included. Q-Tpeak was defined as the interval between QRS onset and the peak of the positive T wave or the nadir of the negative T wave. When the T wave had a biphasic or a notched configuration, the peak of the T wave was defined as that of dominant T deflection. Q-Tend, Q-Tpeak, and Tpeak-end (Q-Tend − Q-Tpeak) as an index of transmural dispersion of repolarization were measured automatically from all 12-lead ECGs, corrected by Bazett's method, and averaged among all 12 leads. Data of corrected Q-Tend, Q-Tpeak, and Tpeak-end, which were measured simply from lead V_5, also were evaluated. As an index of spatial dispersion of repolarization, dispersion of the corrected Q-Tend was defined as the interval between the maximum and the minimum of the corrected Q-Tend among the 12 leads.

Epinephrine administration

A bolus injection of epinephrine (0.1 μg/kg) was immediately followed by continuous infusion (0.1 μg/kg/min). The 12-lead ECG was continuously recorded during sinus rhythm under baseline conditions and usually for 5 minutes under epinephrine infusion. The effect of epinephrine on both RR and QT intervals usually reached steady-state conditions 2 to 3 minutes after the start of epinephrine infusion. Epinephrine infusion for >5 minutes was avoided, and ECG monitoring was continued for another 5 minutes after epinephrine infusion to detect the possible occurrence of torsades de pointes. The ECG data as a representative of the peak epinephrine effect were collected 1 to 2 minutes after the start of epinephrine infusion when the RR interval was the shortest, whereas the data as a representative of the steady-state epinephrine effect were collected 3 to 5 minutes after the start of epinephrine infusion.

Statistical analysis

Data are expressed as mean ± SD, except for those shown in Figure 3, which are expressed as mean ± SEM. Repeated-measures two-way ANOVA followed by the Scheffé test was used to compare measurements made before and after epinephrine infusion and to compare differences between groups (STATISTICA, 98 Edition). Repeated-measures one-way ANOVA followed by the Scheffé test was used to compare changes (Δ) in the measurements with epinephrine between groups. Differences in frequencies were analyzed by Chi-square test. A two-sided $P < .05$ was considered statistically significant.

Results

Retrospective study

Best ECG criteria to differentiate LQT1, LQT2, LQT3, and Control groups

The retrospective study as well as our previous study[12] suggested the differential response of the mean corrected Q-Tend interval to epinephrine test among LQT1, LQT2, and LQT3 groups. The mean corrected Q-Tend intervals were more prominently prolonged at peak epinephrine effect in LQT1 and LQT2 groups than in either the LQT3 or the Control group. On the other hand, they remained pro-

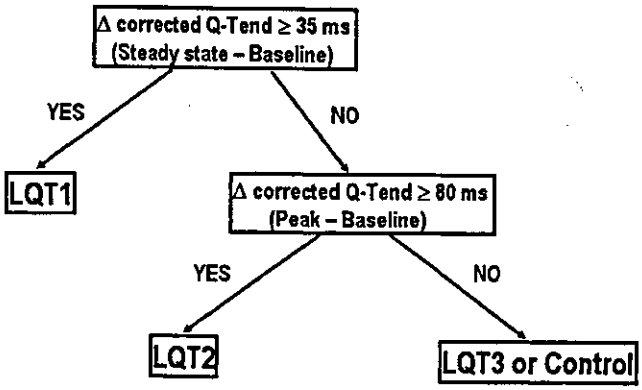

Figure 1 Flow chart for predicting genotype with the epinephrine test.

longed at steady-state epinephrine effect only in the LQT1 group but not in the other three groups.

Figure 1 illustrates a flow chart for predicting LQT1, LQT2, LQT3, and Control patients with the epinephrine test derived from the retrospective study. If the Δ mean corrected Q-Tend was ≥35 ms at steady-state epinephrine effect, the patient was expected to be affected with LQT1 syndrome. If not, and the Δ mean corrected Q-Tend was ≥80 ms at peak epinephrine effect, the patient was expected to be linked to LQT2 syndrome. If not, the patient was expected to be an LQT3 or Control patient.

Prospective study

Differential responses of ECG parameters to epinephrine infusion

Figure 2 illustrates ECG lead V_4 under baseline conditions and at peak and steady-state epinephrine effects in representative LQT1, LQT2, LQT3, and Control patients.

Figure 3 shows composite data of the ECG parameters under baseline conditions and at peak and steady-state epinephrine effects in the four groups of the prospective study. Under baseline conditions, the mean corrected Q-Tend and Q-Tpeak were significantly longer in the LQT1, LQT2, and LQT3 groups than in the Control group; both were significantly longer in the LQT2 and LQT3 groups than in LQT1 group (Figure 3A and 3B). The mean corrected Tpeak-end was significantly greater in the LQT2 group than in the LQT3 or Control group (Figure 3C). The dispersion of corrected Q-Tend was significantly larger in the LQT1 and LQT2 groups than in the Control group (Figure 3D). The mean corrected Q-Tend and Q-Tpeak were dramatically prolonged at peak epinephrine effect (470 ± 41 to 596 ± 56 ms, 385 ± 34 to 480 ± 53 ms; $P < .05$, respectively) and remained prolonged at steady state (549 ± 55 ms, 438 ± 50 ms; $P < .05$ vs baseline, respectively) in the LQT1 group (Figure 3A and 3B, closed circles). The mean corrected Tpeak-end also was markedly increased at peak epinephrine effect (85 ± 11 to 115 ± 19 ms; $P < .05$), and remained increased at steady state (111 ± 17 ms; $P < .05$ vs baseline) as a result of a greater prolongation in the mean corrected

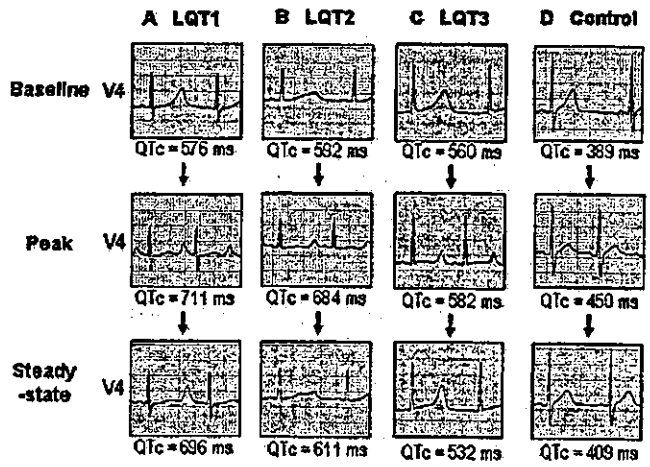

Figure 2 ECG lead V_4 under baseline conditions and at peak and steady-state epinephrine effects in LQT1 (A), LQT2 (B), LQT3 (C), and Control (D) patients. The mean corrected Q-Tend was prominently prolonged from 576 to 711 ms at peak epinephrine effect and remained prolonged at steady state (696 ms) in the LQT1 patient. In the LQT2 patient, the mean corrected Q-Tend also was dramatically prolonged from 592 to 684 ms at peak but returned to the baseline level at steady-state (611 ms). It was much less prolonged (LQT3: 560 to 582 ms, Control: 389 to 450 ms) at peak in the LQT3 and Control patients than in either the LQT1 or LQT2 patient and was shortened to the baseline level at steady state (532, 409 ms).

Q-Tend than in the mean corrected Q-Tpeak at both peak and steady-state conditions (Figure 3C, closed circles). The mean corrected Q-Tend and Q-Tpeak also were dramati-

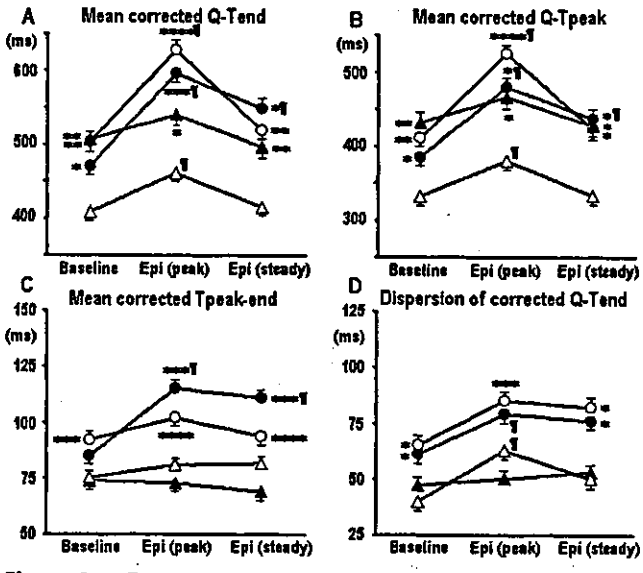

Figure 3 Composite data of the mean corrected Q-Tend (A), Q-Tpeak (B), Tpeak-end (C), and dispersion of corrected Q-Tend (D) under baseline conditions and at peak and steady-state epinephrine effects in LQT1 *(closed circle)*, LQT2 *(open circle)*, LQT3 *(closed triangle)*, and Control *(open triangle)* groups of the prospective study. *$P < .05$ vs Control; **$P < .05$ vs LQT1 and Control; ***$P < .05$ vs LQT3 and Control; ****$P < .05$ vs LQT1, LQT3, and Control; ¶$P < .05$ vs baseline.